FMH606 Master's Thesis 2023

Master of Science, Electrical Power Engineering

Solar Power in Wind Power Park – Evaluating flexible power generation based on real and simulated data from Statkraft Smøla Wind Park

Andreas Dolven Jacobsen

Faculty of Technology, Natural sciences and Maritime Sciences
Campus Porsgrunn

Course: FMH606 Master's Thesis, 2023

Title: Solar Power in Wind Power Park – Evaluating flexible power generation based on real and simulated data from Statkraft Smøla Wind Park

Number of pages: 46

Keywords: Solar power, wind power, co-location, correlation analysis, power production, Smøla, Norway

Student: Andreas Dolven Jacobsen

Supervisor: Nils Jakob Johannesen

External partner: **COWI**

Summary:

Meeting future energy and environmental demands poses new challenges, with one of them being the uncertainty and variability in power production from renewable energies such as solar and wind power due to their dependency on weather, causing them to be referred to as intermittent energy sources. At the island of Smøla in Norway there is currently a wind park with an installed wind capacity of 150.4 MW. This report will look into the complementary characteristics of co-locating solar and wind power at Smøla by finding the optimal mix of solar and wind power for a larger capacity wind turbine that may be installed after the end of life of the current wind turbines. The optimal mix is adjusted in order to maximize the usage of the transmission line capacity that connects Smøla to the mainland, while keeping the curtailed power below a given percentage. The complementary characteristics will also be analysed using correlation analysis with Pearson's r correlation factor calculated at hourly, daily and monthly resolution. To accomplish this, irradiance and wind data was gathered from openly available sources, and then calculating solar power using models from literature and wind power with power curves for the specified wind turbine models. The power production calculations and correlation analysis were performed using python, and the power production scenarios was optimized using the excel optimization toolbox. The power production scenarios presented for the years 2017-2020 shows that by only installing the larger wind turbines results in 2824 GWh of power being delivered to Nordheim with an average transmission line usage of 56 % and 140 GWh of power being curtailed. With both solar and wind power the power delivered to Nordheim was 3105 GWh with wind power accounting for 85 % of the power produced and solar with 15 %. The average transmission line usage was 61.5 % and 163 GWh of power was curtailed. The correlation analysis shows that the complementary characteristics for solar and wind power calculated across the year is strongest for monthly timelines with a correlation factor of -0.58, which decreases as the resolution gets finer, with daily resolution being -0.34 and hourly resolution with -0.15.

Preface

This report constitutes the master's thesis in the Electrical Power Engineering program at the University of South-Eastern Norway (USN). Thanks to both USN and COWI/IFE for the opportunity to write a thesis on renewable energy sources such as wind and solar power.

Porsgrunn, 15.05.2023

Andreas Dolven Jacobsen

Contents

Nomenclature

This nomenclature presents a list of symbols and a list of abbreviations and terms used in this report.

Symbols

The following is a list of symbols used in this report:

Symbol	Explanation
A	Area, $[m^2]$
$\epsilon_{curtailed}$	Percentage threshold on power that can be curtailed, [%]
η_{nom}	Nominal power of the solar module at standard testing conditions, $[W/m^2]$
η_{rel}	Solar module efficiency relative to efficiency at standard testing conditions, $[-]$
η_T	Fractional loss from transmission of wind power, $[-]$
η_{tot}	Efficiency of the wind turbine system, $[-]$
G	Irradiance hitting the solar panel surface, $[W/m^2]$
G'	Normalized irradiance hitting the solar module, $[-]$
G_{STC}	Irradiance hitting the solar panel under standard testing conditions, $[W/m^2]$
i	Numerator of observations, $[-]$
k_1-k_6	Coefficients related to a particular solar module material, $[-, -, {}^\circ C^{-1}, {}^\circ C^{-1}, {}^\circ C^{-1}, {}^\circ C^{-2}]$
n	Total number of observations, $[-]$
n_B	Total number of Bonus B76/2000 wind turbines, $[-]$
n_{MWp}	Installed solar capacity, $[MWp]$
n_s	Total number of Siemens SWT-2.3-82 wind turbines, $[-]$
$n_{S,4.0}$	Number of Siemens SWT-4.0-130 wind turbines, $[-]$
P_{AC}	Power produced as AC, $[W]$
P_{DC}	Power produced as DC, $[W]$

P_e	Electrical power output gained from wind, $[W]$
$P_{e,r}$	Electrical power output gained from wind at rated wind speed, $[W]$
P_W	Theoretical power that can be gained from wind, $[W]$
P_B	Interpolated power for Bonus B76/2000 wind turbine, $[W]$
$P_{consumed}$	Power consumed at Smøla, $[W]$
$P_{curtailed}$	Power curtailed due to transmission line limit, $[W]$
P_{lim}	Power limit of the transmission line, $[W]$
$P_{Nordheim}$	Power delivered to Nordheim, $[W]$
$P_{produced}$	Power produced from the solar farm and wind farm at Smøla, $[W]$
P_S	Interpolated power for Siemens SWT-2.3-82 wind turbine, $[W]$
$P_{S,4.0}$	Power produced from the Siemens SWT-4.0-130, $[W]$
$P_{Smøla}$	Power delivered to and from Smøla, $[W]$
P_{SN}	Power delivered specifically in the direction of Smøla to Nordheim, $[W]$
P_{solar}	Solar power produced, $[W]$
$P_{solar,MWp}$	Solar power produced per MWp every hour, $[W/MWp]$
$P_{turbine}$	Individual power from wind turbines by interpolation from power curve data points, $[W]$
P_{wind}	Wind power produced from power curve of wind turbine, $[W]$
r	Pearson's r correlation coefficient
R	Radius, $[m]$
$r_{x,y}$	Pearson's r correlation coefficient of input data set x and y
ρ	Density of air, $[kg/m^3]$
T_a	Ambient temperature, $[^\circ C]$
T_m	Temperature of the solar module, $[^\circ C]$
T_{STC}	Temperature under standard testing conditions, $[^\circ C]$

TL_{usage}	Average percentage usage of transmission line, [%]
U_0	Coefficient for type of installation of the solar module, $[W/(^{\circ}C \cdot m^2)]$
U_1	Coefficient for type of installation of the solar module, $[(W \cdot s)/(^{\circ}C \cdot m^3)]$
W	Wind speed, $[m/s]$, used for wind speeds at varying height levels
W_c	Cut-off wind speed where the wind turbine will not be able to produce power, $[m/s]$
W_f	Furling wind speed where the wind turbine is shutdown to avoid damages, $[m/s]$
W_r	Rated wind speed where the turbine produces its rated power, $[m/s]$
x	Observations of data ''x'' as input to the Pearson's r correlation coefficient, units dependent on data.
y	Observations of data ''y'' as input to the Pearson's r correlation coefficient, units dependent on data.

Abbreviations and terms

The following is a list of abbreviations and terms used in this report:

Abbr/term	**Explanation**
AC	Alternate-current
COWI	International consulting firm
Curtailment	Power loss by withholding power production due to system limitations.
DC	Direct-current
IEC	International Electrotechnical Commision
IFE	Institutt For Energiteknikk (Institute for Energy Technology)
MERRA2	Modern-Era Retrospective Analysis for Research and Applications, Version 2 (MERRA2) is an openly available climate database produced by NASA's Global Modelling and Assimilation Office (GMAO).
Meteonorm	Commercial software giving access to various weather data and calculation tools, and is a product developed by Meteotest AG.

Renewables Ninja	An openly available database providing weather and energy data for solar and wind. It was created by the authors of [1] and [2], and uses their methods for estimating solar power with the GSEE model (Global Solar Energy Estimator) in [1] and for wind power the VWF model (Virtual Wind Farm) in [2]. [3] Ninja renewables uses MERRA2 and CM-SAF SARAH as weather sources.
PVcase	Commercial software developed by PVcase for planning and designing utility scale solar power plants.
PVGIS	Photovoltaic Geographical Information System (PVGIS) is an openly available online tool giving access to information about solar radiation and photovoltaic system performance. PVGIS is developed by the Joint Research Centre (JRC) – European Commision.
PVGIS-SARAH2	Surface Solar Radiation Data Set – Heliosat (SARAH) – Edition 2 is developed by the European Organisation for the Exploitation of Meteorological Satelittes (EUMETSAT) at the Satellite Application Facility on Climate Monitoring (CM SAF). PVGIS-SARAH2 is derived from SARAH2 from EUMETSAT - CM SAF.
PVsyst	Commercial software developed by PVsyst for simulating power production of solar power plants.
TSO	Transmission system operator

1 Introduction

This introductory chapter covers the background, objectives, methods, scope, and lastly the report structure of this report.

1.1 Background

The need for renewable and environmentally friendly energy sources must meet future energy demands and environmental concerns. The problem with renewable energy sources such as wind and solar power is that they are not always available due to their dependency on the variability of weather, making them an intermittent energy source. When they are available the power demand might not be there, leading to various energy storage solutions. Uncertainty in weather forecasts also makes it difficult to reliably schedule power to the transmission system operator (TSO). At the island of Smøla in Norway there is a wind farm with installed capacity of 150.4 MW, with a transmission line leading to the mainland having a capacity of 160 MVA. In this report the focus will be if co-locating solar and wind power at Smøla can complement each other by improving the usage of the transmission line and provide power more reliably. Previous work on Smøla in [4] regarding co-locating solar and wind power focused on the current installation of wind turbines. Another suggestion mentioned in [4] was to install larger wind turbines after the end-of-life of the current wind turbines. This report will therefore look into power production scenarios regarding installation of larger wind turbines at Smøla, together with solar power and look into the complementary characteristics of co-locating these two renewable energy sources by the use of correlation analysis.

1.2 Objective

This report intends to simulate solar power and wind power to investigate their complementary characteristics by:

- Evaluating power production scenarios with larger wind turbines installed at Smøla without and in combination with solar power.
- Performing a correlation analysis between the solar power and wind power for the specified location of Smøla, Norway.

Given that measured wind power produced at Smøla has been made available for the period 2017-2020, a comparison between simulated solar power with either simulated or measured wind power has been performed for both the objectives above to gauge possible inaccuracies in the result.

1.3 Methods

Data for irradiance has been gathered from Photovoltaic Geographical Information System (PVGVIS) - Surface Solar Radiation Data Set – Heliosat Edition 2 (SARAH2) in [5] and solar power has been calculated using the method presented by PVGIS in [6], which references [7] as the source of the model. Wind speeds is gathered from Ninja Renewables in [3], which extrapolates the wind speeds from Modern-Era Retrospective Analysis for Research and Applications, Version 2 (MERRA2) using the virtual wind farm model in [2]. The wind speeds are then used to calculate the wind power by using the power curves of the wind turbine models. The calculation of produced power and correlation analysis has been performed in python. For evaluating power production scenarios the produced solar and wind power is exported to excel

in order to use the excel optimization toolbox. The balance between installed capacity of solar and wind power is then optimized given restriction on transmission line capacity and curtailed power to maximize the total power delivered, hence maximizing transmission line usage.

1.4 Scope and limitations

This report is limited to evaluating power production and performing a correlation analysis at Smøla in order to determine the complimentary characteristics of co-locating solar and wind power. It does not intend to look into the positives or negatives regarding economics or environment, nor provide a technical solution given the power production scenarios. A limiting factor for assessing power production by installing a larger capacity wind turbine at Smøla has been the limited availability of power curves for wind turbines, especially for newer models. The correlation analysis by itself does not explain the cause for why there might be a correlation between two variables, and it will be considered outside the scope of this report to analyse meteorological phenomenon that can represent the cause.

1.5 Report structure

In Chapter 2 a system description is given of Smøla with a simplified overview of the power system. A literature review is conducted in Chapter 3 regarding optimal mixing of solar and wind power and their complementary characteristics with the use of correlation analysis. Relevant theory regarding calculation of solar power, wind power and correlations analysis is given in Chapter 4. In Chapter 5 and 6 the methodology is presented for evaluating power production and for performing the correlation analysis. In Chapter 7 the results are presented, and a discussion of the results is given in Chapter 8. Chapter 9 presents the conclusion of this report with mentions future work.

2 System description

This chapter presents information about the location Smøla where the wind farm is situated and is where the solar farm has been proposed to be built. Description and details about the existing wind farm and the proposed solar farm is also presented.

2.1 Smøla

Smøla is an island located in Norway in the county of Møre and Romsdal and the island has an approximate land area of 216 km^2. [8] The county Møre and Romsdal is marked in black in the map of Norway in Figure 2.1, with a closer view in Figure 2.2, which also shows an outline of the location of Smøla in the upper right.

Figure 2.1: Map of Norway with the county Møre and Romsdal marked in black. [9]

Figure 2.2: Outline of Møre and Romsdal with the location of Smøla outlined in the upper right. [10]

2.2 Wind farm

The wind farm at Smøla is located at approximately 63.400 ºN and 7.9300 ºE, as marked in Figure 2.3, which also shows outlined areas of nature reserves at Smøla:

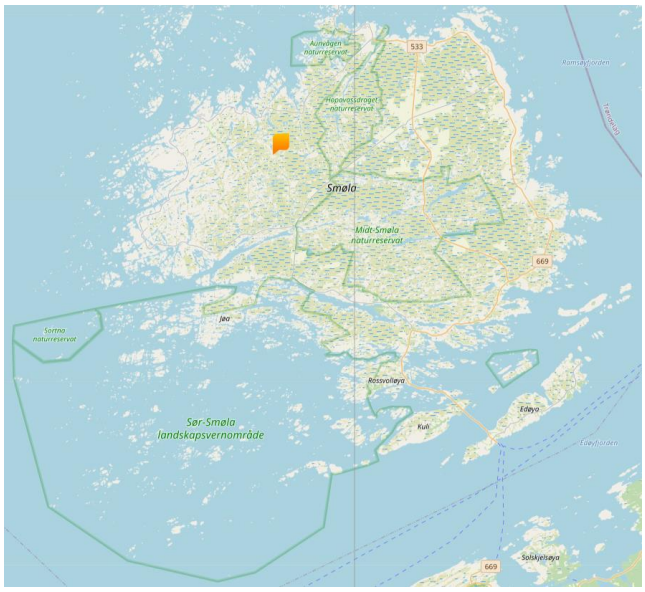

Figure 2.3: Smøla with approximate location of the wind farm and outlined areas of various nature reserves. [11]

The total installed capacity of wind power at Smøla is 150.4 MW, which is comprised of 68 wind turbines in total. The wind farm was built in two stages, first stage in 2001-2002 with a total of 20 wind turbines of Bonus B76/2000 rated at 2.0 MW, and second stage in 2004-2005 with a total of 48 wind turbines of Siemens SWT-2.3-82 rated at 2.3 MW. The tower height of the wind turbines is 70 meters from ground to the hub of the rotor. [12] [13] In Figure 2.4 the distribution of the wind turbines is shown, which has an approximate row spacing of 700-1000 meters with spacing in the rows at 240-350 meters [14] and the area of the park is approximately 18 km^2. Each wind turbine produces power at 690 V, which gets converted to 22 kV by a transformer at the bottom of each wind turbine. The power is then directed to the main transformer station situated roughly in the centre of the park that converts the power from 22 kV to 132 kV and transports it to the mainland through Nordheim, Tutsna. [12] [4]

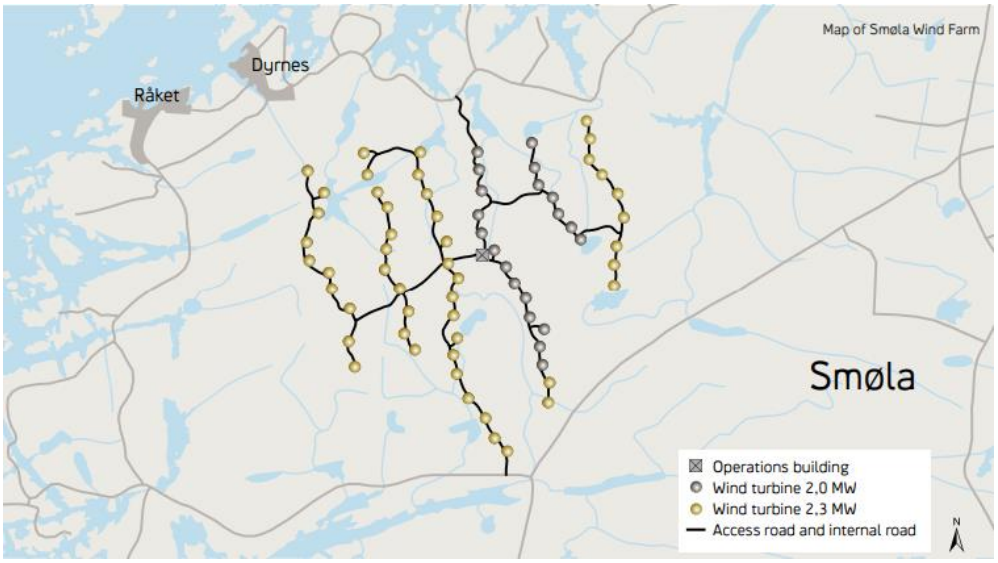

Figure 2.4: Distribution of Bonus B76/2000 2.0 MW and Siemens SWT-2.3-82 2.3 MW wind turbines. [12]

2.3 Solar farm

The solar farm is currently only under consideration for being built at Smøla and therefore doesn't physically exist. In Figure 2.5 is an outline of the area deemed available for building a solar farm, which encompasses more or less the same area as the wind park at 16 km^2. [4]

In [4], COWI and IFE were contracted by the county of Møre and Romsdal to (excluding other topics) evaluate the power production of a solar farm at Smøla and its complementary characteristics with the currently installed wind farm. The power production from a solar farm were evaluated using two different approaches, which both considered a bifacial solar panel:

- A component-based model where components are modelled after physically existing components.
- A coefficient-based model that is modelled after outer variables such as irradiance and cell temperature in relation to the solar power produced under standard testing conditions (STC).

The component-based model used a program called PVcase for placing solar panel components in the area outline in blue in Figure 2.6 of roughly 2.4 km^2, which resulted in an installed solar capacity of 144.9 MWp. The placement was imported into a program called PVsyst for simulating the power produced over the time span of one year with hourly weather data from Meteonorm for the location Jøstølen, Smøla. The result from the installed capacity of 144.9 MWp was scaled up by a factor of 6.29 to represent the entire area of roughly 15 km^2 in

Figure 2.6 giving an installed capacity of 911.4 MWp. The result from the component-based model is presented in Table 2.1, which includes losses in the system such as shadowing of solar panels, ohmic-losses, inverter losses, transformer losses etc, totalling a loss of approximately 25 % up until the main transformer in the park. The coefficient-based model used weather data from PVGIS and was simulated for installed solar capacities of 240 MWp and 911 MWp for the period of 2017-2020, together with measured wind power. The results from the coefficient-based model are also presented in Table 2.1, which used the total loss of 25 % found from the component-based model.

Figure 2.5: Satellite image of Smøla with the outlined area deemed available for installing the solar farm. [4]

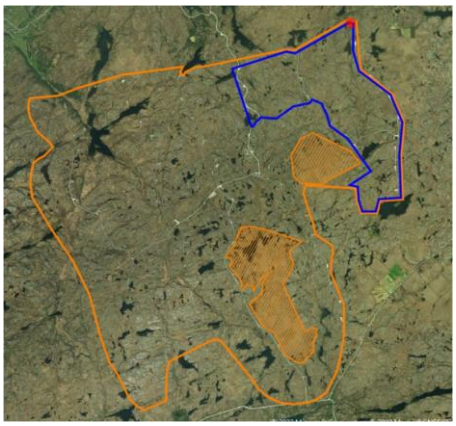

Figure 2.6: Simulated area from [4] outlined in blue with the shaded orange fields deemed unsuitable.

In Table 2.1 is a summary of the results for simulating solar power for the component- and coefficient-based model from [4]. As a simple comparison between the two approaches, by linear interpolation between the installed capacity of 144.9 MWp and 911.4 MWp for the component-based model to an installed capacity of 240 MWp gives 218.6 GWh of solar power. And multiplied by four to represent an equally long time period as the coefficient-based model gives 874.3 GWh solar power as compared to 800 GWh of solar power.

Table 2.1: Summary of power production results from [4].

Metric	Time span [years]	Component-based model		Coefficient-based model	
Installed capacity [MWp]	-	144.9	911.4	240	911
Solar power [GWh]	1	126.2	870.8	N/A	N/A
Solar power [GWh]	4	N/A	N/A	800	2990
Wind power [GWh]	4	N/A	N/A	1250	1250
Total power [GWh]	4	N/A	N/A	2050	4240
Line capacity [MVA]	-	N/A	N/A	160	660
Curtailment [GWh]	4	N/A	N/A	98	65

2.4 Grid connection

The power gets converted from 22 kV to 132kV at the main transformer at Smøla before it gets transferred to the distribution grid at Nordheim, Tutsna. The transmission lines consist of approximately 10 km of ariel cable, 15 km of underground cable and 5 km of sea cable. The maximum capacity of the transmission line is 160 MVA, where it is the underground cable and sea cable that limits the power throughput. [12] [4] In Figure 2.7 is a simplified overview of the distribution network:

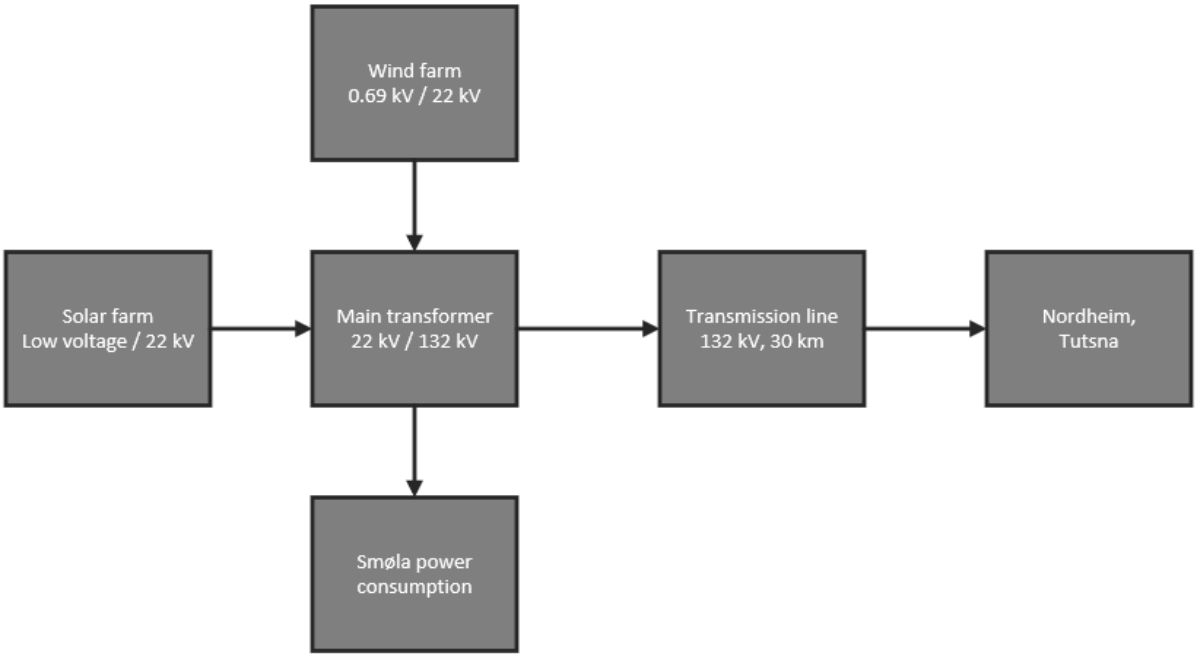

Figure 2.7: Simplified overview of the distribution network.

3 Literature review

This chapter presents a literature review for co-locating solar and wind power regarding optimal mixing of solar and wind from different viewpoints and the complimentary characteristics of solar and wind by the use of correlation analysis.

One of the benefits with taking use of several intermittent renewable energies is to reduce the variability in power production and provide a smoothing effect, including on different timescales such as daily or yearly timelines. Several studies have shown spatial dispersion and co-location solar and wind power can provide a smoothing effect. [15] [16]. Spatial dispersion can provide a smoothing effect on the distribution grid as a whole and co-location can give a local smoothing effect with one of the main benefits being better usage of transmission line capacity. By better utilizing the transmission line capacity the need for enlargement of existing and future electrical infrastructure may be lessened. Other benefits of co-locating solar and wind may include shared operational/control strategies and improved usage of land areas. [17]

The available capacity of solar and wind will vary depending on graphical location, [2] [18] therefore it is decisive for each location to determine the optimal installed capacity of solar and wind power. The optimal solution for installed capacity of solar and wind may consider factors such as generation, transmission, load variations, energy reserves, economics, etc. [19] Several methods have been used for finding optimal solutions such as probabilistic approaches, optimization algorithms and machine learning.

In [20] the balance between solar and wind power across Great Britain was studied by looking into what percentage of solar and wind would reduce the variability in total power output. It was found that seasonal variability was most reduced with 70 % solar power and 30 % wind power, however this was only a hypothetical scenario as it only looked at average production across Great Britain and did not consider load variations or other metrics. A much different approach for balance between solar and wind was looked at in [17], where different ratios of solar and wind was used to determine the best forecast accuracy for the day-ahead market with probabilistic forecasting by the use of machine learning. The ratio that gave the best forecast accuracy constituted of 50 – 60 % wind power and 40 – 50 % solar power.

In both [21] and [22] spatial weather data for wind and solar power was used to determine the optimal mix of installed capacity of solar and wind in Europe by balancing generated power to power demand by minimizing the residual power. In [21] the optimal mix was determined as 74 % wind and 26 %, solar, without considering energy storage. From [22] the optimal mix for balancing power was found to be 90 % wind and 10 % solar, for annual energy balance it was 80 % wind and 20 % solar, while with idealized roundtrip energy storage it was 60 % wind and 40 % solar. In [23] the optimal mix of solar power and wind power was considered for an all-renewable Europe with consideration for energy storage and found the optimal mix to be 55 % wind and 45 % solar.

In [15] a correlation analysis of a future scenario with large-scale solar and wind farms dispersed across Sweden was conducted. The analysis used measured irradiance data from 12 weather stations and wind power data modelled from 56 wind farms at varying locations across Sweden, provided by the Swedish Meteorological and Hydrological Institute. The correlation analysis was performed between the dispersed solar and wind farms, and between produced solar and wind power. The Pearson's r correlation coefficient on a national scale for produced power in co-located solar and wind farms was found to be -0.20 at hourly resolution, -0.46 at daily resolution and -0.74 at monthly resolution. Based on the correlation analysis it was found that both dispersed and combined solar and wind farms can provide a smoothing effect on

power variability. However, the complementary characteristics between solar and wind power is less relevant regarding spatial dispersion, as compared to the individual resource (solar or wind power) being spatially dispersed. These claims are further supported by several studies on this topic referred to in [16], where a scientific review was conducted on assessing the variability and forecasting of renewables such as solar, wind, wave and tidal power. In [15], it is mentioned that it would also be interesting to study the correlation between solar and wind power for local climatic conditions, which is what this report intends to do for the location of Smøla, Norway.

In [24] the complementary characteristics of solar and wind power was studied in the high-latitude artic regions of Northern Norway and Svalbard using correlation analysis. The correlation analysis was conducted at four different locations being Tromsø, Pasvik, Sortland and Ny-Ålesund. The Pearson's r correlation coefficient for these locations were calculated at hourly, daily and monthly resolution. At hourly resolution the correlation coefficient across the year varied between -0.08 to +0.12 for these locations, suggesting no relationship between solar and wind power at this resolution. At daily resolution it varied between -0.07 to -0.26 and at monthly resolution between -0.23 to -0.54, suggesting at most a weak to moderate relationship between solar and wind power. In [20] the complementary variability of solar and wind across Great Britain was studied and found that the Pearson's r correlation coefficient for irradiance and wind speeds varied between -0.20 and -0.40 with generally stronger negative correlation on the west coast of Great Britain, suggesting that locations facing the Atlantic Ocean have generally stronger negative correlation. In more southern parts of Europe such as Italy, it was found from [25] that correlation values on a national scale varied between -0.1 to -0.12 for hourly resolution, -0.39 to -0.43 at daily resolution and -0.61 to -0.65 for monthly resolution.

4 Theory

This theory chapter covers the calculation of solar power, wind power and Pearson's r correlation coefficient.

4.1 Calculation of solar power

The solar generation model to be used is the model used by PVGIS referenced in [6], which again references [7] as the source of the model. In [7] the purpose was to present a general model for photovoltaic power production by irradiance and module temperature. The intention was not to create a more accurate model for simulating photovoltaic power, but to present a model that did not depend on having knowledge about a specifically given solar module and still give results with reasonable accuracy.

The model as presented from [6] calculates the DC power P_{DC} produced by solar modules as:

$$P_{DC} = \frac{G}{G_{STC}} \cdot A \cdot \eta_{nom} \cdot \eta_{rel} \tag{4.1}$$

Where:

- G is the irradiance hitting the solar panel surface, $[W/m^2]$.
- G_{STC} is the irradiance hitting the solar panel under standard testing conditions, $[W/m^2]$.
- A is the total surface area of the solar panel system, $[m^2]$.
- η_{nom} is the nominal power of the solar module at standard testing conditions, $[W/m^2]$.
- η_{rel} is the solar module efficiency relative to efficiency at standard testing conditions, $[-]$

The relative effectiveness η_{rel} is calculated as:

$$\eta_{rel} = 1 + k_1 \, ln(G') + k_2 \, ln(G')^2 + k_3 T' + k_4 T' \, ln(G') + k_5 T' \, ln(G')^2 + k_6 T'^2 \tag{4.2}$$

Where:

- k_1-k_6 are coefficients related to a particular solar module material, $[-, -, \ ^\circ C^{-1}, \ ^\circ C^{-1}, \ ^\circ C^{-1}, \ ^\circ C^{-2}]$
- G' is the normalized irradiance hitting the solar module, $[-]$
- T' is the temperature of the solar module relative to standard testing conditions, $[^\circ C]$

The normalized irradiance G' and temperature T' is calculated as:

$$G' = \frac{G}{G_{STC}} \tag{4.3}$$

$$T' = T_m - T_{STC} \tag{4.4}$$

Where:

- T_m is the temperature of the solar module, $[^\circ C]$.
- T_{STC} is the temperature under standard testing conditions, $[^\circ C]$.

The temperature of the solar modules T_m from [6] is calculated as:

$$T_m = T_a + \frac{G}{U_0 + U_1 \cdot W} \tag{4.5}$$

Where:

- T_a is the ambient temperature, $[°C]$.
- U_0 is a coefficient for type of installation of the solar module, $[W/(°C \cdot m^2)]$.
- U_1 is a coefficient for type of installation of the solar module, $[(W \cdot s)/(°C \cdot m^3)]$.
- W is the wind speed, $[m/s]$.

4.2 Calculation of wind power

The theoretical power that can be gained from wind P_W can be calculated as: [26]

$$P_W = \frac{1}{2} \cdot \pi R^2 \cdot W^3 = \frac{1}{2} \rho A W^3 \tag{4.6}$$

Where:

- ρ is the density of air, $[kg/m^3]$.
- A is the area that is swept by rotor blades of the turbine, $[m^2]$.
- W is the wind speed, $[m/s]$.

However due to losses the electrical output power P_e can be given as: [26]

$$P_e = \frac{1}{2} \eta_{tot} \rho A W^3 \tag{4.7}$$

Where η_{tot} represent the overall all efficiency of the wind turbine system, which may include losses such as turbine efficiency, gearbox efficiency and generator efficiency. The electrical power output P_e for a given type of manufactured turbine is often represented with a power curve as shown in Figure 4.1 with electrical power output P_e as a function of wind speed W. In Figure 5.5 the wind speed W_c is the cut-off wind speed where the wind turbine will not be able to produce power, at the rated wind speed W_r the turbine produces its rated power $P_{e,r}$ and at wind speeds above the furling wind speed W_f the wind turbine is shutdown to avoid damages. [26] It is important to note that between the wind speeds W_r and W_f there is a system in place such as brakes or turbine blade pitching to keep the turbine rotating at the rated speed, otherwise there is a continuous drop in power output above the wind speed W_r. [27] The power produced from wind will be calculated using the power curves of the wind turbine models specified in this report.

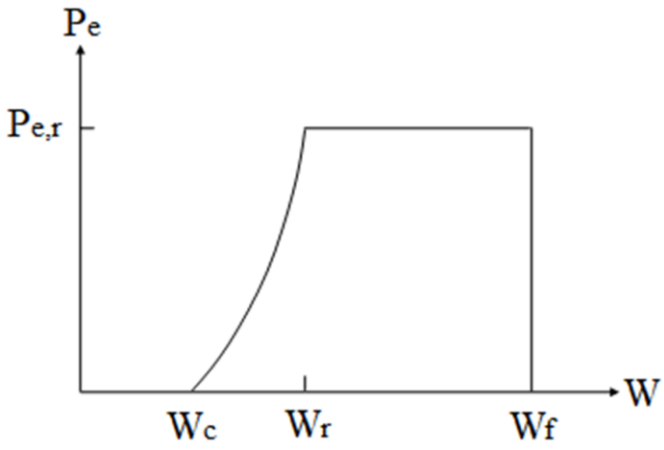

Figure 4.1: Example of wind turbine power curve. [26]

4.3 Correlation analysis

The purpose of correlation analysis is to determine the type of relationship between two variables without going into the details of cause and effect surrounding the change in the variables themselves. The types of relationships are categorized as: [28]

- Positive correlation: When one of the variables increases the other variable tends to also increase.
- Weak or no correlation: There is little to no observable relationship between the change in the variables.
- Negative correlation: When one of the variables increases the other tends to decrease.

The strength of the relationship is also determined in correlation analysis given by the correlation coefficient, which assumes a value in the range [-1, 1], where -1 or 1 equals perfect negative or positive correlation and 0 refers to no correlation. There are several methods for calculating a correlation coefficient and the choice of method may depend on factors such as linearity or non-linearity of the variables, independence testing of variables and so forth. A common method for linear correlation is the Pearson's r correlation coefficient calculated as: [28]

$$r_{xy} = \frac{n\sum x_i y_i - \sum x_i \sum y_i}{\sqrt{n\sum x_i^2 - (\sum x_i)^2}\sqrt{n\sum y_i^2 - (\sum y_i)^2}} \tag{4.8}$$

Where:

- r_{xy} is the Pearson's r correlation coefficient of x and y
- n is the number of total observations i
- x_i is the value of x at observation number i
- y_i is the value of y at observation number i

In Figure 4.2 and Figure 4.3 is an example of perfect negative and positive correlation visualized using a scatter plot with x_i versus y_i:

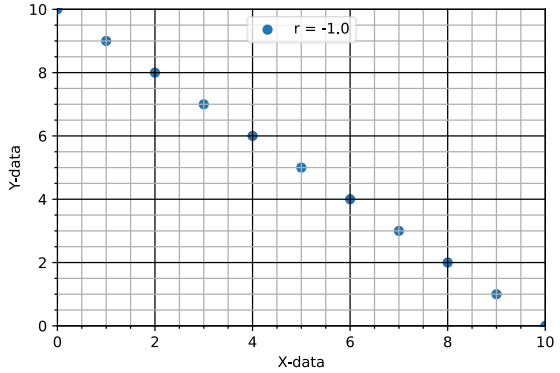

Figure 4.2: Example of perfect negative correlation using scatter plot of x_i versus y_i.

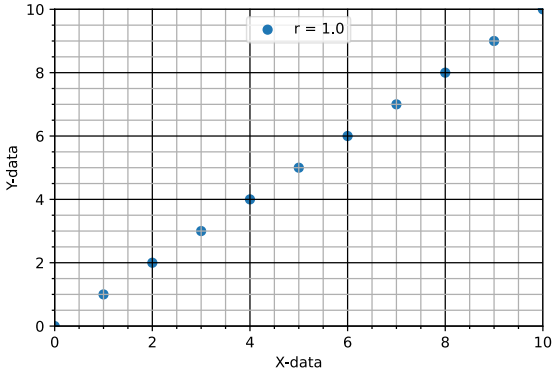

Figure 4.3: Example of perfect positive correlation using scatter plot of x_i versus y_i.

5 Evaluating power production

This chapter presents the methods used for calculating power produced from solar and wind, a simplified overview and calculation of the power flow in the system and the optimization of power production scenarios. The calculation of wind power presents the calculation with symbols for the current set of wind turbines at Smøla and the switch to the larger capacity wind turbine is presented later in subchapter 5.4. In Figure 5.1 is an overview of the scenarios that will be presented in subchapter 5.4 in order to evaluate the power production at Smøla.

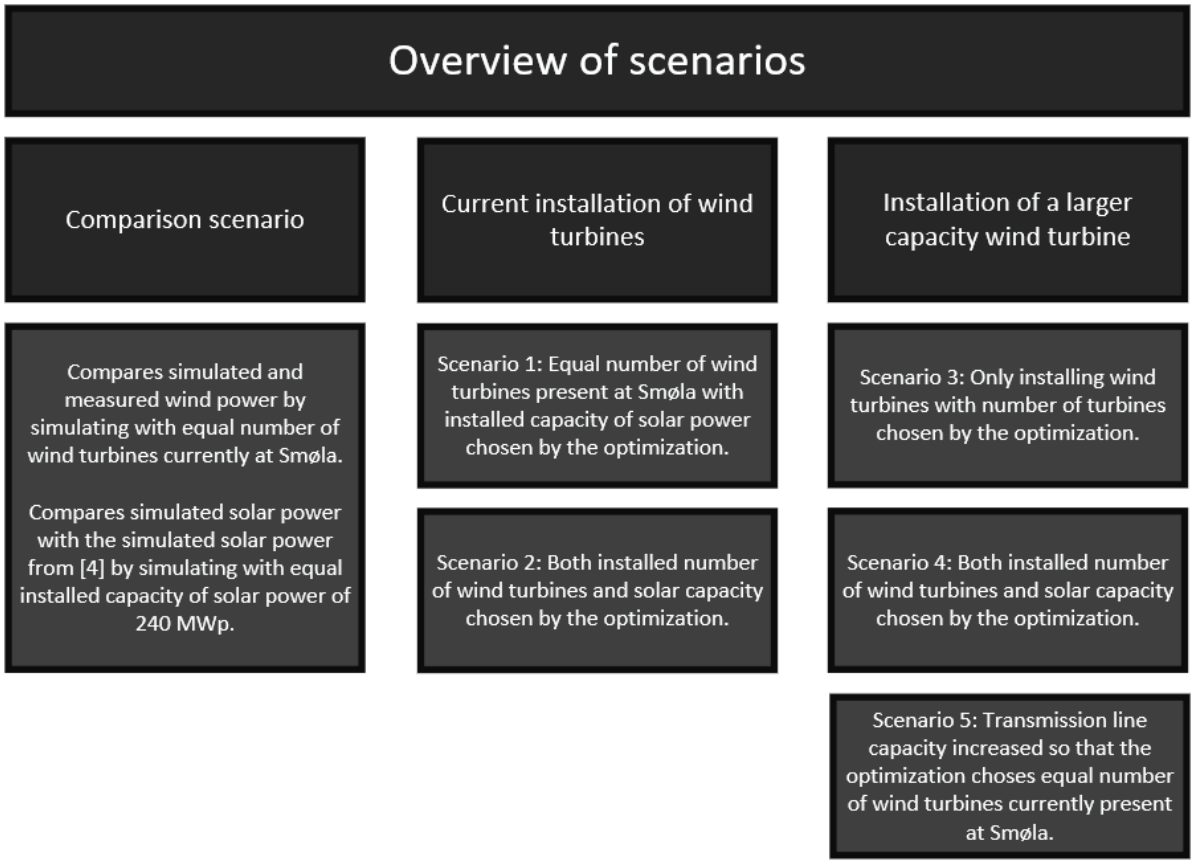

Figure 5.1: Overview of scenarios for evaluating power production at Smøla.

5.1 Simulating solar power

The solar power P_{DC} is calculated using the equations (4.1) to (4.5) presented in Chapter 4. The data input for irradiance G was gathered from the PVGIS online tool in [5] using PVGIS-SARAH2 database with hourly resolution for the years 2017 – 2020 at coordinates 63.400 ^{o}N and 7.9300 ^{o}E. The irradiance data gathered from [5] had the slope and azimuth angle optimized for a fixed-mounted solar panel to respectively 45˚ and 3˚. The data set also contains input for ambient temperature T_a and wind speed W for equation (4.5). The irradiance G is plotted in Figure 5.2, ambient temperature T_a in Figure 5.3 and wind speed W in Figure 5.4:

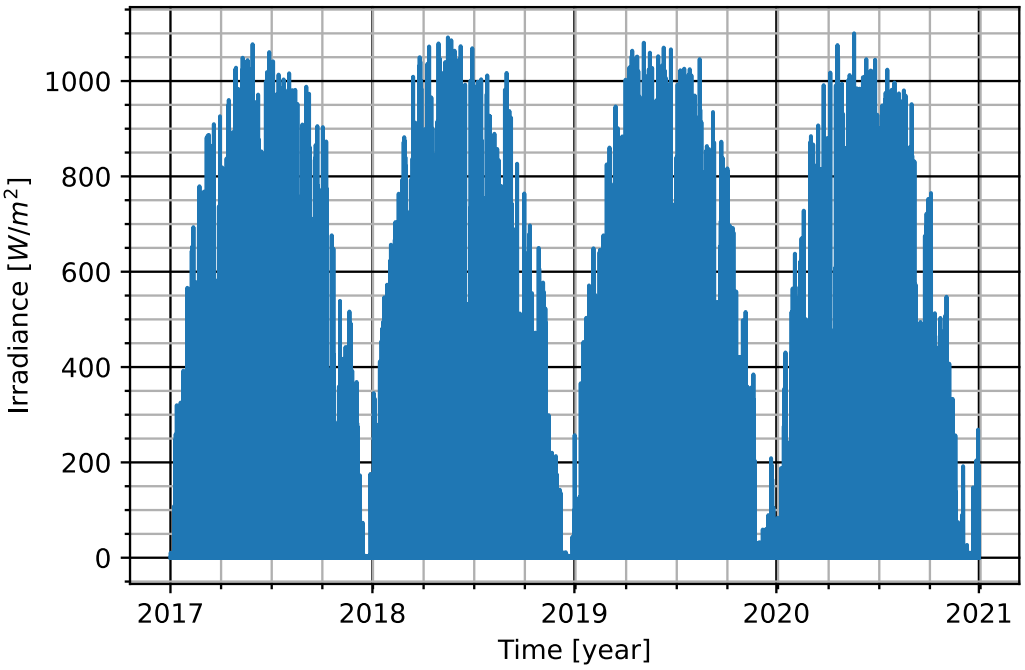

Figure 5.2: Plot of irradiance G gathered from [5].

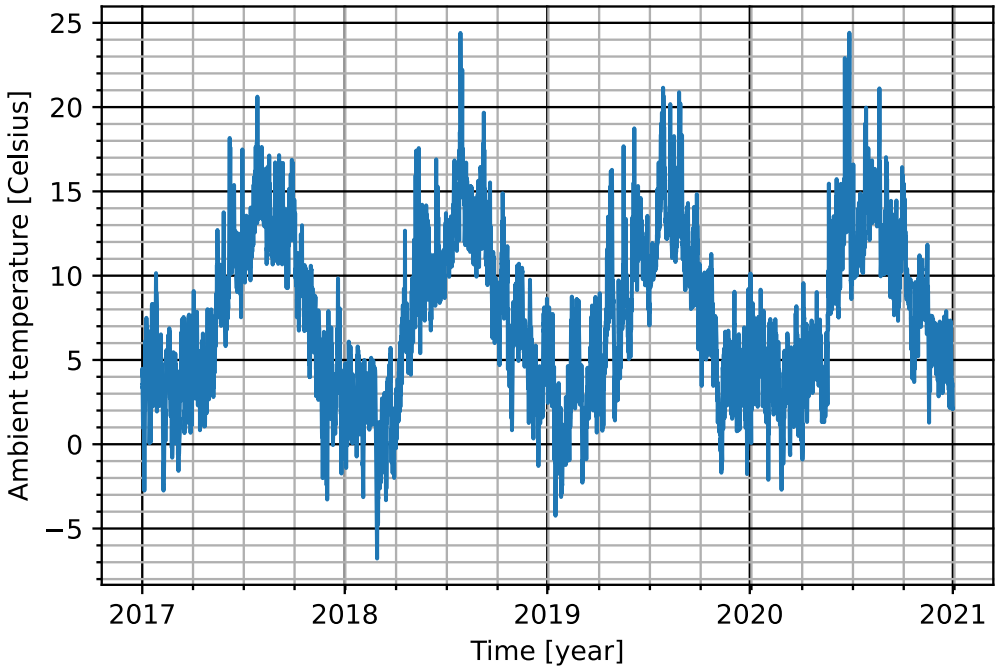

Figure 5.3: Plot of ambient temperature T_a at 2 meter height, gathered from [5].

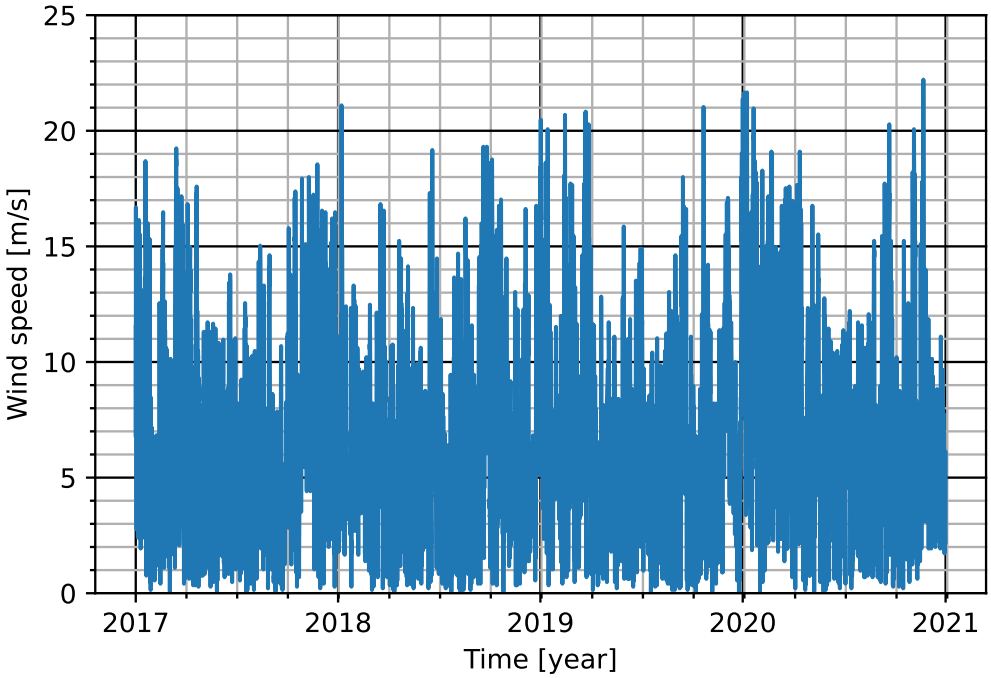

Figure 5.4: Plot of wind speeds W at 10 meter height, gathered from [5].

The coefficients k_1-k_6 in equation (4.2) are based on the type of material used for the solar panel. The material crystalline-Silicon (c-Si) has been selected and the coefficients are gathered from PVGIS in [6] and presented in Table 5.1:

Table 5.1: Coefficients for calculating η_{rel}. [6]

Coefficient	k_1	k_2	k_3	k_4	k_5	k_6
Value	-0.017237	-0.040465	-0.004702	0.000149	0.000170	0.000005

The coefficients U_0 and U_1 in equation (4.5) are based on solar panel material, which has been selected as c-Si and the type of installation is chosen as free-standing. The coefficients U_0 and U_1 are gathered from PVGIS in [6] and presented in Table 5.2:

Table 5.2: Coefficient for calculating solar panel temperature T_m. [6]

Coefficient	U_0	U_1
Value	26.9	6.2

The DC power P_{DC} produced from equation equations (4.1) to (4.5) is converted to AC power P_{AC} transmitted to the high voltage side of the main transformer at 22 kV by using the power loss of 25 % found in [4]. The solar power $P_{solar,i}$ for every i-th hour is then calculated as:

$$P_{solar,i} = P_{AC,i} = 0.75 \cdot P_{DC,i}$$

Where $P_{DC,i}$ is the DC power calculated at every hour i given inputs of irradiance G_i, temperature $T_{a,i}$ and wind speed W_i.

5.2 Simulating wind power

To simulate wind power the power curves of the wind turbines installed at Smøla will be used, which gives the electrical power output as a function of wind speed. This subchapter will focus on calculating wind power with the current wind turbines at Smøla, while the switch to a larger capacity wind turbine is presented in subchapter 5.4. The model of the wind turbines used at Smøla is the Siemens SWT-2.3-82 and Bonus B76/2000. Data points for their power curves was obtained from [29] for increments of 0.5 m/s of wind speeds, which is presented in Figure 5.5:

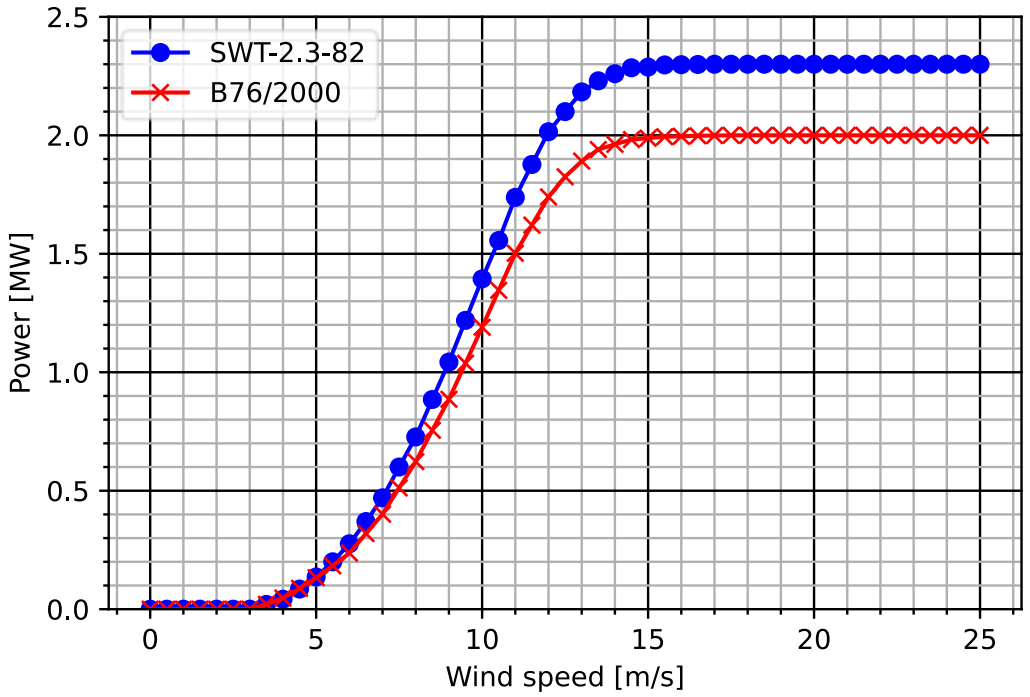

Figure 5.5: Power curves for Siemens SWT-2.3-82 and Bonus B76/2000 wind turbines.

Data for wind speeds at Smøla was gathered for the coordinates 63.400 ºN and 7.9300 ºE from [3], which uses the MERRA2 database with an hourly resolution. In [3] the wind speeds from MERRA2 have been extrapolated to present wind speeds for wind turbine hub heights in the range 10-150 m. Wind speeds were gathered for the years 2017-2020 for the hub height at 70 m for the Siemens SWT-2.3-82 and Bonus B76/2000 wind turbines. The wind speeds are presented in Figure 5.6:

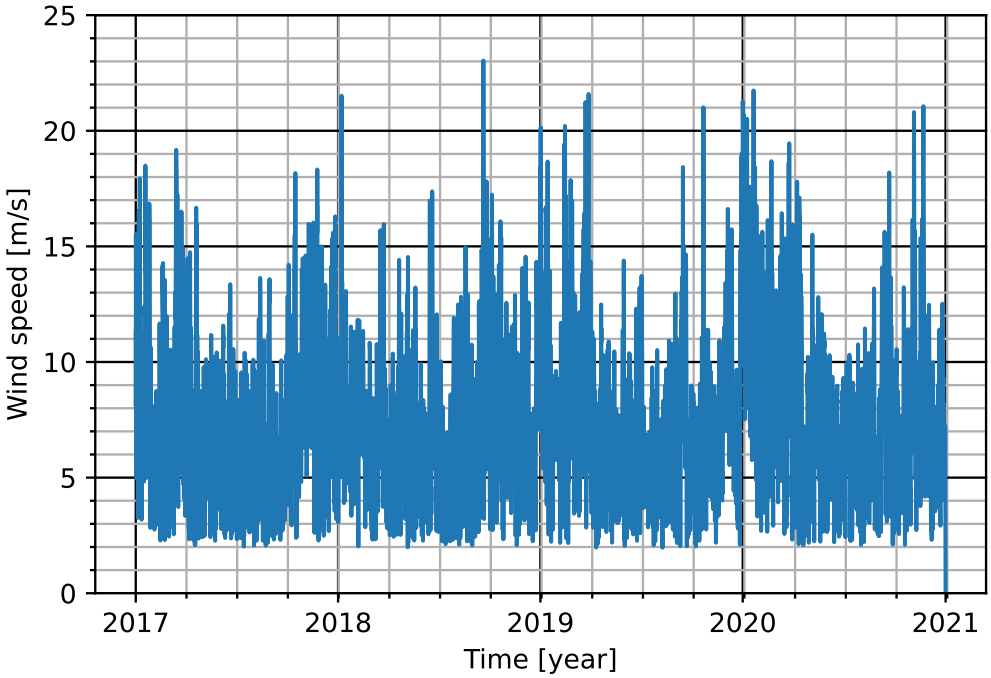

Figure 5.6: Extrapolated wind speeds from Merra2 gathered from [3].

With the wind speeds the power output is calculated using the power curve data points by performing linear interpolation to smooth out the curve:

$$P_{turbine,i} = P_1 + (W_i - W_0)\frac{P_1 - P_0}{W_1 - W_0} \tag{5.1}$$

Where:

- $P_{turbine,i}$ is the interpolated power of a specified wind turbine at the i-th hour, $[W]$.
- W_i is the wind speed at the i-th hour at the hub height of the wind turbine, $[m/s]$.
- W_0 and W_1 is the wind speeds from the power curve that is lower and higher than the wind speed W_i, $[m/s]$.
- P_0 and P_1 is the power corresponding to the wind speeds W_0 and W_1 from the power curve, $[W]$.

The wind power for every hour $P_{wind,i}$ is then calculated as:

$$P_{wind,i} = n_S P_{S,i} + n_B P_{B,i} \tag{5.2}$$

Where:

- n_s is the total number of Siemens SWT-2.3-82 wind turbines, $[-]$.
- P_S is the interpolated power for Siemens SWT-2.3-82 wind turbine, $[W]$.
- n_B is the total number of Bonus B76/2000 wind turbines, $[-]$.
- P_B is the interpolated power for Bonus B76/2000 wind turbine, $[W]$.

Measurements of power production from Smøla delivered to Nordheim across the 160 MV transmission line have been made available for the years 2017-2020. Using these measurements, the fractional loss from transmission η_T is estimated by taking the peak power delivered at any time, which turns out to be approximately 147.9 MW and calculate the loss from the installed capacity of the wind turbines at 150.4 MW:

$$\eta_T = \frac{\text{Peak power}}{\text{Installed capacity}} = \frac{147.9}{150.4} \approx 0.98$$

The calculated fractional loss η_T from transmission also includes the transmission across the 132 kV transmission line, however it will be assumed negligible so that the calculated wind power is the power delivered right after being converted from 22 kV to 132 kV. This assumption is done so that the total power produced at Smøla at the main transformer of the park can simply assume the sum of solar and wind power produced. The total wind power every hour $P_{wind,i}$ is then calculated as:

$$P_{wind,i} = \eta_T \cdot \left(n_S P_{S,i} + n_B P_{B,i}\right) \tag{5.3}$$

5.3 Power flow

The total power being produced from the solar and wind farm at Smøla $P_{produced}$ is given by:

$$P_{produced} = P_{solar,i} + P_{wind,i} \tag{5.4}$$

At Smøla there is also power being consumed locally, which varies between 3-7 MW and hourly measurements are only available for the year 2021. Data points starting from 24.03.23 to 13.06.23 were missing measurements, totalling 480 data points, which have been estimated by taking the average of 480 data points before and after this occurrence. There were also a few ‘’error’’ measurements, which were removed and interpolated. These changes can be viewed from the unmodified data plotted in Figure 5.7 to the modified data in Figure 5.8:

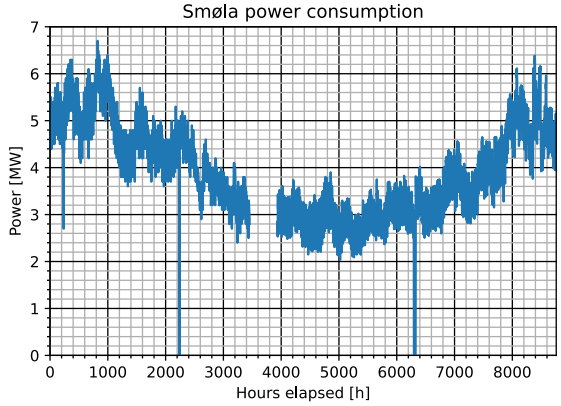

Figure 5.7: Unmodified power consumption at Smøla.

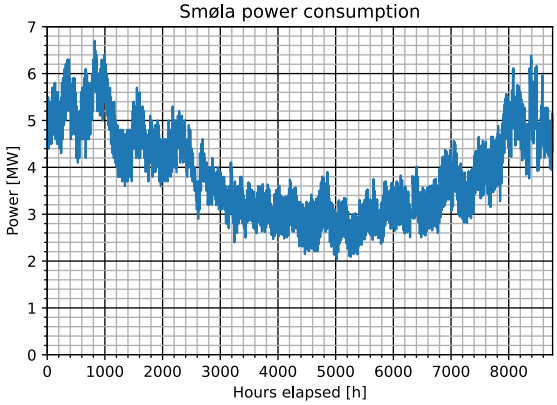

Figure 5.8: Modified power consumption at Smøla.

The modified power consumption at Smøla for the year 2021 has been applied to every year for the simulated period of 2017-2020. The total power delivered to the 132 kV transmission line at every hour $P_{Smøla,i}$ is then given by:

$$P_{Smøla,i} = P_{solar,i} + P_{wind,i} - P_{consumed,i} \tag{5.5}$$

Due to the solar and wind farm not always producing more power than what is consumed at Smøla, the power flow specifically in the direction of Nordheim $P_{SN,i}$ can be described by:

$$P_{SN,i} = \begin{cases} P_{solar,i} + P_{wind,i} - P_{Smøla,i}, & P_{solar,i} + P_{wind,i} \geq P_{Smøla,i} \\ 0, & P_{solar,i} + P_{wind,i} < P_{Smøla,i} \end{cases} \tag{5.6}$$

Given a limit on transmission line capacity from Smøla to Nordheim, the curtailed power $P_{curtailed,i}$ due to the transmission line limit P_{lim} is given by:

$$P_{curtailed,i} = \begin{cases} P_{SN,i} - P_{lim}, & P_{SN,i} \geq P_{lim} \\ 0, & P_{SN,i} < P_{lim} \end{cases} \quad (5.7)$$

The total power delivered to Nordheim, $P_{Nordheim,i}$, is then simply given as:

$$P_{Nordheim,i} = P_{SN,i} - P_{curtailed,i} \quad (5.8)$$

Which assumes lossless transmission across the transmission line. And the percentage usage of the transmission line capacity TL_{usage} is calculated as:

$$TL_{usage} = \frac{\sum_i^n P_{Nordheim,i}}{n \cdot P_{lim}} \cdot 100\% \quad (5.9)$$

The power flow is visualized using the simplified overview of the distribution network presented in Chapter 2 in Figure 5.9:

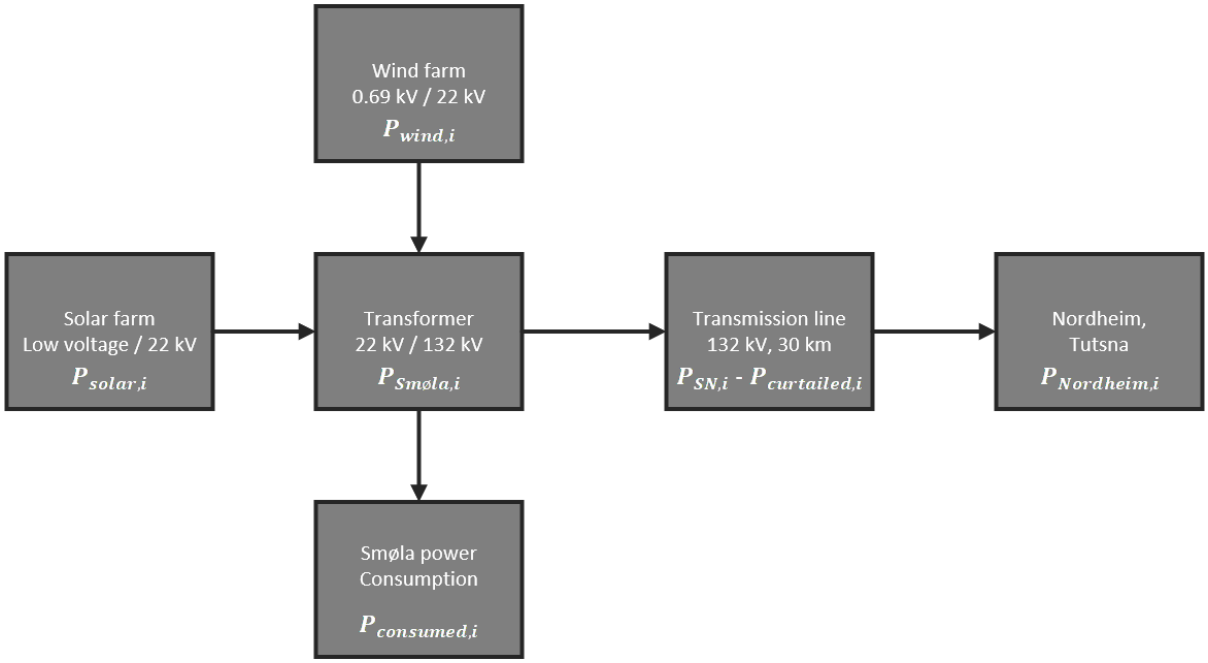

Figure 5.9: Simplified overview of the distribution network with power flows indicated.

5.4 Power production scenarios

The power production is first evaluated by a comparison scenario comparing the simulated wind power and measured wind power together with solar power in order to gauge the magnitude of which simulated wind power may under- or overestimate the power produced. This comparison uses equal amount of wind turbines installed at Smøla of Siemens SWT-2.3-82 and Bonus B76/2000, and an installed solar capacity of 240 MWp to compare with the solar power produced from [4]. The measured wind power is measured at Nordheim, and the measured wind power presented as $P_{wind,i}$ is therefore estimated by performing the calculation of $P_{Nordheim,i}$ in subchapter 5.3 in reverse, excluding the term $P_{solar,i}$. This does underestimate the measured wind power presented as $P_{wind,i}$, due to the curtailed power $P_{curtailed,i}$ for these

measurements being unknown. This way of representing the produced measured wind power, $P_{wind,i}$, is also applied for the correlation analysis in chapter 6. For this scenario plots are also produced for simulated solar power, simulated wind power, measured wind power and total power with either simulated or measured wind power for the period of 2017-2020.

The goal with co-locating solar and wind power is to take advantage of their complimentary characteristics, such as improved utilization of the distribution network capacity. At Smøla the transmission line is a limiting factor in terms curtailment, which limits the installed capacity of either solar power and/or wind power that can be delivered to the mainland at Nordheim. Therefore, further scenarios will seek to maximize the utilization of the transmission line by finding the optimal values for installed capacity of solar and wind power. This has been done by using the optimization toolbox in excel, where the objective function becomes to maximize the power delivered to Nordheim:

$$maximize = \sum_{i}^{n} P_{Nordheim,i} \tag{5.10}$$

Where $P_{Nordheim}$ is calculated as in subchapter 5.3. The solar power has been calculated as the power produced per MWp every hour and for wind power the power produced is calculated per wind turbine for every hour before being exported from python to excel. Therefore, the equation for $P_{solar,i}$ and $P_{wind,i}$ in the excel optimization may be presented as:

$$P_{solar,i} = P_{solar,i,MWp} \cdot n_{MWp} \tag{5.11}$$

$$P_{wind,i} = n_S P_{S,i} + n_B P_{B,i} \tag{5.12}$$

Where:

- $P_{solar,i,MWp}$ is the solar power produced per MWp every hour, $[W/MWp]$.
- n_{MWp} is the installed solar capacity, $[MWp]$.

And the remaining expressions is as presented previously. The constraint for maximizing the power delivered across the transmission line is constrained by keeping the curtailed power below a chosen percentage $\epsilon_{curtailed}$ of total power delivered in the direction of Nordheim before curtailment $P_{SN,i}$, expressed as:

$$P_{curtailed} \leq \epsilon_{curtailed} \cdot \sum_{i}^{n} P_{SN,i} \tag{5.13}$$

Where $P_{curtailed}$ and $P_{SN,i}$ is calculated as in subchapter 5.3. The variables in this optimization are the installed solar power n_{MWp} taking float values and the installed number of turbines n_S and n_B taking integer values, with all of them being non-negative. In some of the scenarios these variables will instead be set as a parameter to view different options, which does make the use of an optimization algorithm somewhat redundant for some of the scenarios, but for consistency all of the scenarios are performed using the excel optimization toolbox. Given the objective function the problem is a continuous non-linear problem and therefore the generalized reduced gradient (GRG) nonlinear method is chosen in excel.

In all scenarios the acceptable power loss percentage $\epsilon_{curtialed}$ is set to 5 %. The transmission line capacity limit P_{lim} is set to 144 MW by assuming a power factor of 0.9 for the 160 MVA limit of the transmission line at Smøla, unless specified otherwise.

Firstly, the optimization is focused on the current installation of wind turbines by the following scenarios:

- Scenario 1: Change in variable n_{MWp}, with n_S and n_B set as parameters with values equal to current number of installed wind turbine for each model.
- Scenario 2: Change in variables n_{MWp}, n_S and n_B.

Further scenarios will focus on the installation of a larger capacity wind turbine after the end-of-life of the currently installed wind turbines. The chosen turbine is the Siemens SWT-4.0-130 rated at 4.0 MW, which is an older model that's no longer in production, but this model was chosen due to lack of openly available power curve data of newer wind turbine models. In Figure 5.10 is a comparison between the power curves of the current wind turbines at Smøla versus the Siemens SWT-4.0-130. It can be seen from the comparison in Figure 5.10 that the SWT-4.0-130 wind turbine has better characteristics by having a lower cut-off wind speed W_c and rated wind speed W_r, while still having equal furling speed W_f.

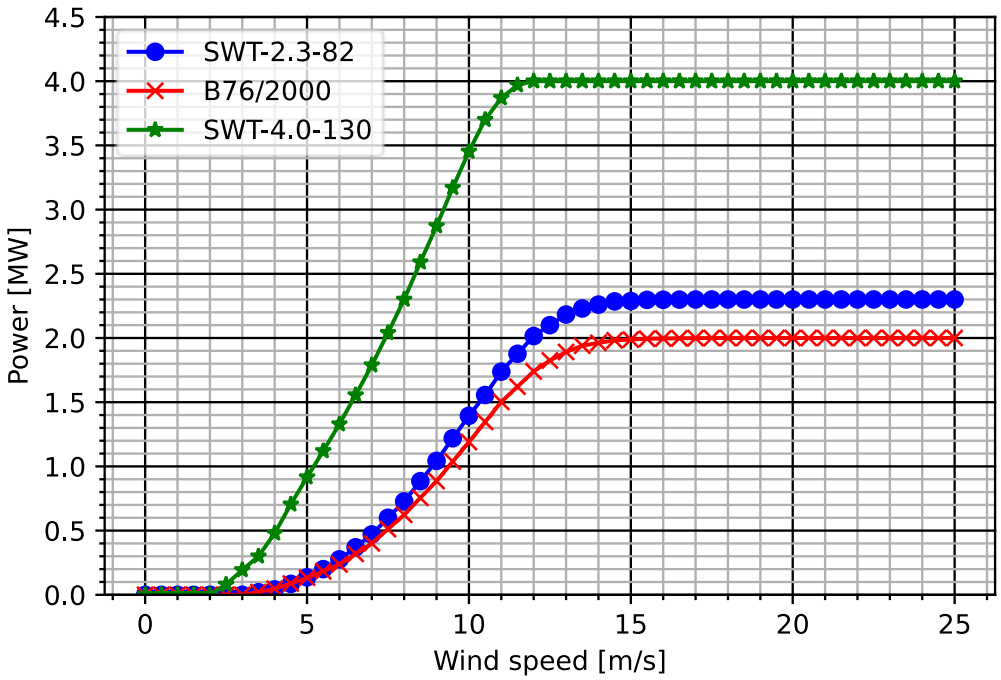

Figure 5.10: Power curves of Siemens SWT-2.3-82, Bonus B76/2000 and Siemens SWT-4.0-130.

The hub height for the Siemens SWT-4.0-130 seems to be only listed as site specific from viewing archived brochures of the model produced by Siemens at [30]. After viewing brochures of wind turbines with similar rotor diameter (130 m) such as the SWT-2.3-120 at [31] and the newer model series Siemens Gamesa (SG) rated at 4 - 5 MW from [32], a hub height of approximately 85 meters seems reasonable. The wind data at 70 m is then replaced by wind data for the hub height of 85 m from [3].

With this turbine the produced wind power $P_{wind,i}$ is calculated as:

$$P_{wind,i} = \eta_T n_{S,4.0} P_{S,4.0,i} \tag{5.14}$$

Where:

- $n_{S,4.0}$ is the number of Siemens SWT-4.0-130 wind turbines, $[-]$.
- $P_{S,4.0,i}$ is the power produced every i-th hour of the Siemens SWT-4.0-130, $[W]$.

With these changes the scenarios being optimized are:

- Scenario 3: Change in variable $n_{S,4.0}$, with n_{MWp} as a parameter set to zero in order to compare power production without solar power present.
- Scenario 4: Change in variable $n_{S,4.0}$ and n_{MWp}.
- Scenario 5: Change in variable $n_{S,4.0}$ and n_{MWp}, with the parameter for transmission line capacity limit P_{lim} changed to a value that results in the optimization choosing $n_{S,4.0} = 68$ (current number of installed wind turbines). This was done through trial and error by changing the value of P_{lim} and running the optimization.

6 Correlation analysis

This chapter presents how the correlation analysis between wind and solar power has been conducted and showcases the scatter plots for simulated values of $P_{solar,i}$ versus $P_{wind,i}$ in order to view the possibility of negative correlation being present.

The correlation analysis is performed using the Pearson's r correlation coefficient as described in equation (4.8), where the inputs x_i and y_i is the solar power $P_{solar,i}$ and wind power $P_{wind,i}$. The calculation of the correlation coefficient is performed with the inputs $P_{solar,i}$ and $P_{wind,i}$ being either at hourly, daily or monthly resolution. Daily and monthly resolution is simply the sum of the input at all the hours within the daily or monthly timeframe. At hourly and daily resolution the Pearson's r correlation coefficient is calculated for every month of the year and for monthly resolution correlation coefficient is calculated only once across the entire year. Given that the inputs span the years 2017-2020, when calculating the correlation for individual months the specific month in question is concatenated for the years 2017-2020.

In Figure 6.1 to Figure 6.3 scatter plots of $P_{solar,i}$ and $P_{wind,i}$ is plotted at hourly, daily and monthly resolution. When comparing these figures to the example of perfect negative and positive correlation in Figure 4.2 and Figure 4.3, it seems reasonable to expect some negative correlation to occur due to a downward trend from top left to bottom left of the plots in Figure 6.1 to Figure 6.3.

A graphical presentation of the correlation has also been presented using plots. In these plots the correlation coefficient r has been calculated for every day of the year using a forward span of n number of days for each day. This has been performed at hourly and daily resolution with spans of 30 and 90 days, resulting in four plots in total.

For comparison, the correlation for simulated solar power and simulated wind power has been presented together with the correlation between simulated solar power and measured wind power.

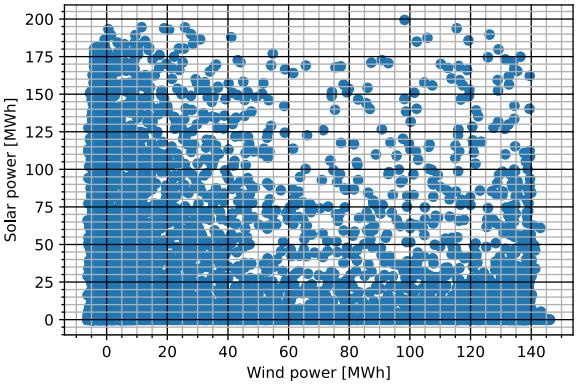

Figure 6.1: Scatter plot of $P_{solar,i}$ and $P_{wind,i}$ at hourly resolution.

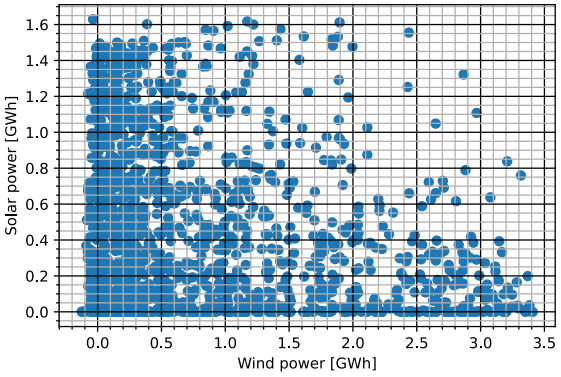

Figure 6.2: Scatter plot of $P_{solar,i}$ and $P_{wind,i}$ at daily resolution.

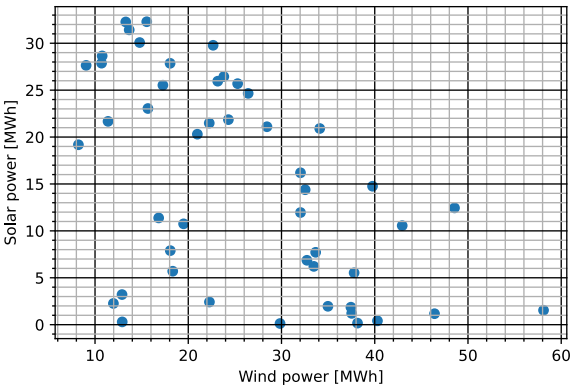

Figure 6.3: Scatter plot of $P_{solar,i}$ and $P_{wind,i}$ at monthly resolution.

7 Results

This chapter presents the results from the power production scenarios and correlation analysis.

7.1 Power production scenarios

The figures from Figure 7.1 to Figure 7.5 represents the power produced for the comparison scenario. In Figure 7.1 is the simulated solar power from a 240 MWp solar farm for the years 2017 to 2020 and the total power produced in this period is approximately 725 GWh:

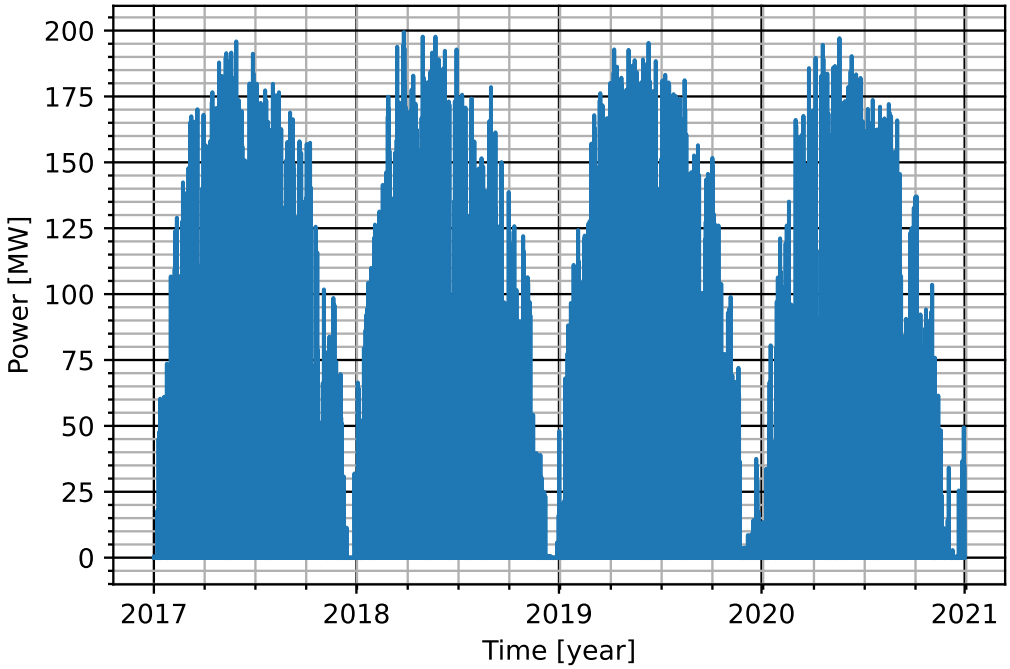

Figure 7.1: Simulation of solar power produced by a 240 MWp solar farm.

In Figure 7.2 is the simulated wind power for the current installation of wind turbines for the years 2017 to 2020 and the total power produced in this period is approximately 1633 GWh:

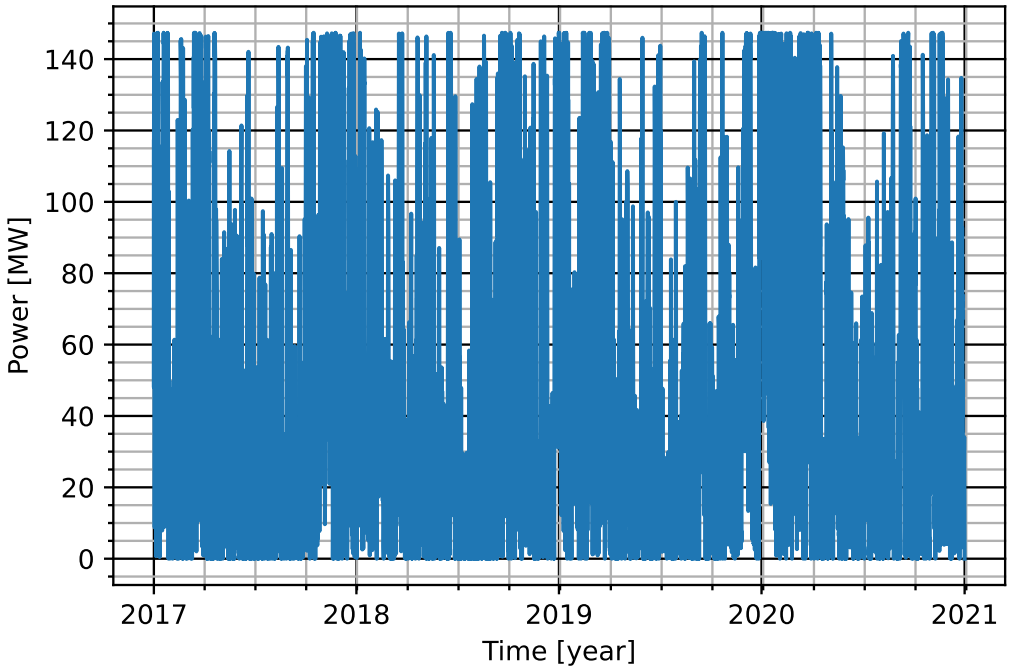

Figure 7.2: Simulated wind power from power curves of Siemens SWT-2.3-82 and Bonus B76/2000 wind turbines and equal number of wind turbines situated at Smøla.

Total power produced from simulated solar and wind power is presented in Figure 7.3, with the orange line indicating the capacity limit of the 160 MVA transmission line at 0.9 PF. The total power produced from both solar and wind is then approximately 2358 GWh.

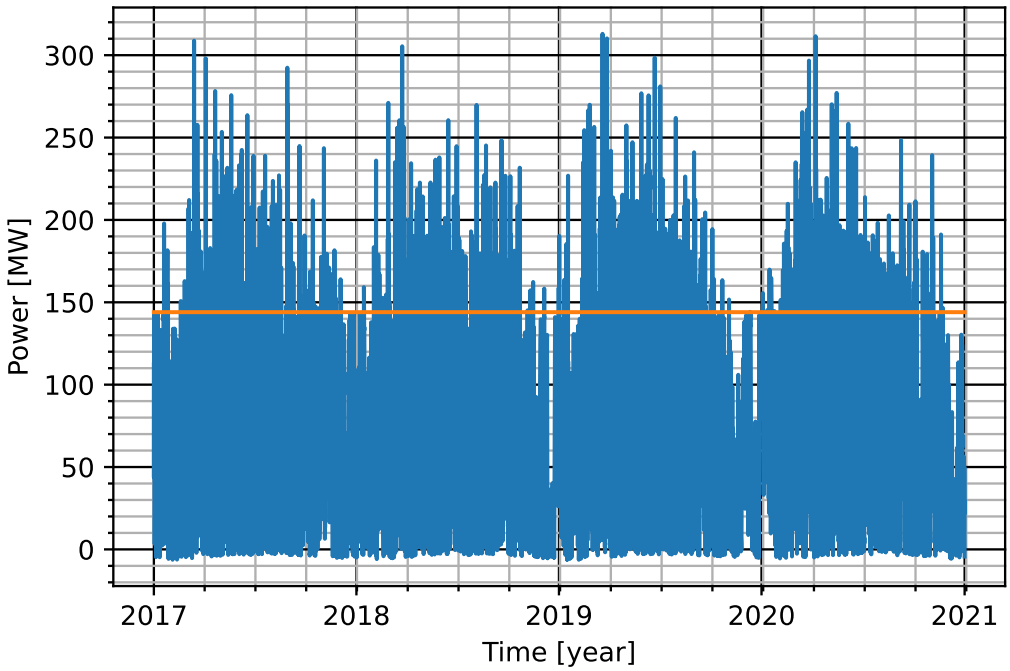

Figure 7.3: Total simulated power produced by the solar and wind farm, with a line marking the maximum capacity of the transmission line assuming 0.9 PF of the 160 MVA capacity.

In Figure 7.4 is the measured production of wind power estimated from measurements at Nordheim for the years 2017 to 2020 and the total wind power produced in this period is approximately 1357 GWh:

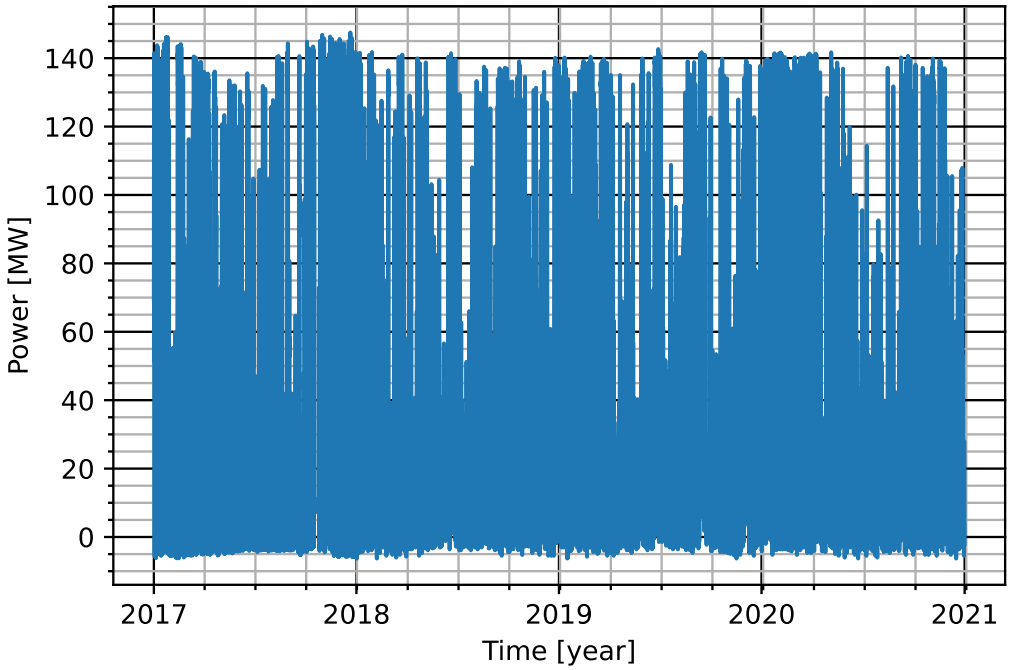

Figure 7.4: Measured wind power at Nordheim in the period 2017 to 2020.

Total power produced by simulated solar and measured wind power is presented in Figure 7.5, with the orange line indicating the transmission line capacity limit of 160 MVA at 0.9 power factor. The total power production from simulated solar power and measured wind power is approximately 2082 GWh.

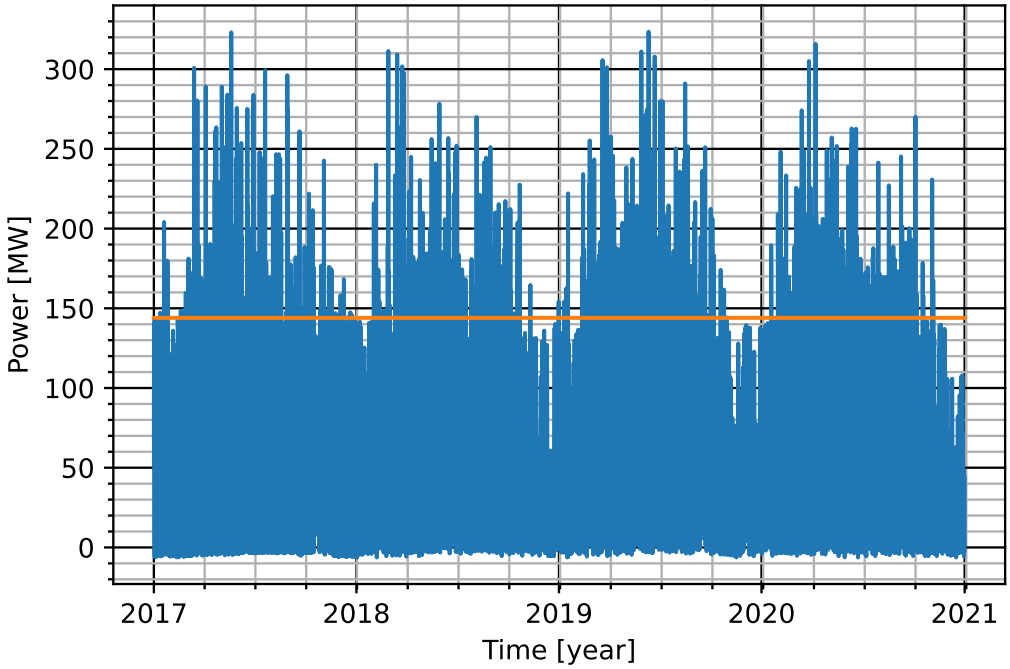

Figure 7.5: Total simulated solar power and measured wind power, with a line indicating maximum capacity of the transmission line assuming 0.9 PF of the 160 MVA capacity.

In Table 7.1 is a summary of the comparison scenario with the power flows presented in subchapter 5.3:

Table 7.1: Summary of power production from a simulated 240 MWp solar farm, with either simulated or measured wind power with installed capacity of 150.4 MW.

	Simulated solar power and simulated wind power	Simulated solar power and measured wind power
P_{solar}	725 GWh (31 % of $P_{produced}$)	725 GWh (35 % of $P_{produced}$)
P_{wind}	1633 GWh (69 % of $P_{produced}$)	1357 GWh (65 % of $P_{produced}$)
$P_{produced}$	2358 GWh	2082 GWh
$P_{Smøla}$	2220 GWh	1945 GWh
P_{SN}	2225 GWh	1964 GWh
$P_{curtailed}$	86.7 GWh (3.9 % of P_{SN})	97.6 GWh (5.0 % of P_{SN})
$P_{Nordheim}$	2139 GWh	1866 GWh
TL_{usage}	42.4 %	37.0 %

In Table 7.2 is the results of Scenario 1 and 2 presented in subchapter 5.4, which focuses on the current installation of wind turbines:

Table 7.2 Optimized scenarios of current installation of wind turbines for Scenario 1 and 2 presented in subchapter 5.4.

	Scenario 1	Scenario 2
Variables	$n_{MWp} = 261$	$n_{MWp} = 215$ $n_S = 74$ $n_B = 0$
Parameters	$n_S = 48$ $n_B = 20$ $\epsilon_{curtailed} = 5\%$ $P_{lim} = 144\ MW$	$\epsilon_{curtailed} = 5\%$ $P_{lim} = 144\ MW$
P_{solar}	788 GWh (33 % of $P_{produced}$)	650 GWh (26 % of $P_{produced}$)
P_{wind}	1633 GWh (67 % of $P_{produced}$)	1850 GWh (74 % of $P_{produced}$)
$P_{produced}$	2421 GWh	2500 GWh
$P_{Smøla}$	2284 GWh	2362 GWh
P_{SN}	2289 GWh	2367 GWh
$P_{curtailed}$	114 GWh	118 GWh
$P_{Nordheim}$	2174 GWh	2250 GWh
TL_{usage}	43.0 %	44.6 %

In Table 7.3 is the results for Scenario 3, 4, and 5 presented in subchapter 5.4, which focuses on the larger capacity wind turbine:

Table 7.3: Optimized scenarios for installing the larger capacity wind turbine SWT-4.0-130 according to Scenario 3, 4 and 5 presented in subchapter 5.4.

	Scenario 3	Scenario 4	Scenario 5
Variables	$n_{S,4.0} = 43$	$n_{S,4.0} = 40$ $n_{MWp} = 172$	$n_{S,4.0} = 68$ $n_{MWp} = 284$
Parameters	$n_{MWp} = 0$ $\epsilon_{curtailed} = 5\%$ $P_{lim} = 144\ MW$	$\epsilon_{curtailed} = 5\%$ $P_{lim} = 144\ MW$	$\epsilon_{curtailed} = 5\%$ $P_{lim} = 245\ MW$
P_{solar}	0 GWh (0 % of $P_{produced}$)	520 GWh (15 % of $P_{produced}$)	858 GWh (15 % of $P_{produced}$)
P_{wind}	3101 GWh (100 % of $P_{produced}$)	2885 GWh (85 % of $P_{produced}$)	4905 GWh (85 % of $P_{produced}$)
$P_{produced}$	3101 GWh	3405 GWh	5764 GWh
$P_{Smøla}$	2964 GWh	3268 GWh	5627 GWh
P_{SN}	2965 GWh	3269 GWh	5627 GWh
$P_{curtailed}$	140 GWh	163 GWh	281 GWh
$P_{Nordheim}$	2824 GWh	3105 GWh	5345 GWh
TL_{usage}	56.0 %	61.5 %	62.0 %

7.2 Correlation between wind and solar power

In Table 7.4 is a comparison of Pearson's r correlation factor for simulated solar power with either simulated wind power or measured wind power:

Table 7.4: Comparison of Pearson's r correlation factor between simulated solar power and either simulated wind power or measured wind power at hourly, daily and monthly resolution.

Time span	Simulated solar power and simulated wind power			Simulated solar power and measured wind power		
	Hourly	Daily	Monthly	Hourly	Daily	Monthly
Jan	-0.13	-0.46	-	-0.11	-0.45	-
Feb	-0.08	-0.14	-	-0.08	-0.19	-
Mar	-0.13	-0.37	-	-0.10	-0.40	-
Apr	-0.20	-0.53	-	-0.16	-0.50	-
Mai	-0.10	-0.26	-	-0.02	-0.19	-
Jun	-0.08	-0.28	-	-0.01	-0.19	-
Jul	-0.11	-0.19	-	-0.04	-0.09	-
Aug	-0.12	-0.32	-	-0.03	-0.08	-
Sep	-0.22	-0.46	-	-0.17	-0.44	-
Oct	-0.16	-0.33	-	-0.11	-0.29	-
Nov	-0.06	-0.13	-	-0.07	-0.12	-
Dec	-0.02	-0.09	-	-0.02	-0.08	-
Full year	-0.18	-0.38	-0.63	-0.11	-0.30	-0.53

In Figure 7.6 to Figure 7.9 is a comparison of correlation coefficient between simulated solar power with either simulated or measured wind power. In Figure 7.6 the span is 30 days using hourly resolution, in Figure 7.7 the span is 90 days using hourly resolution, in Figure 7.8 the span is 30 days using daily resolution and in Figure 7.9 the span is 90 days using daily resolution. For clarification, reading off a point a point on the plotted lines indicates the expected correlation read from the y-axis for the next n number of days spanned at the corresponding point on the x-axis.

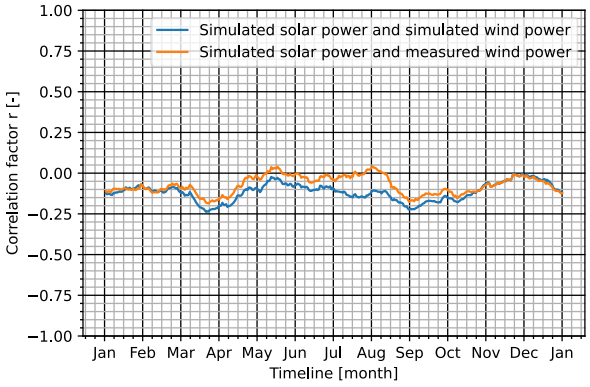

Figure 7.6: Correlation coefficient calculated at spans of 30 days for each day of the year using hourly resolution.

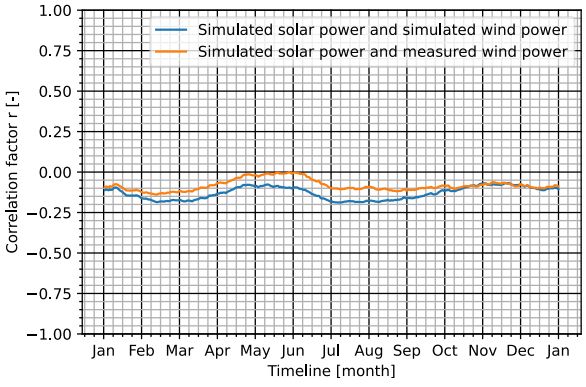

Figure 7.7: Correlation coefficient calculated at spans of 90 days for each day of the year using hourly resolution.

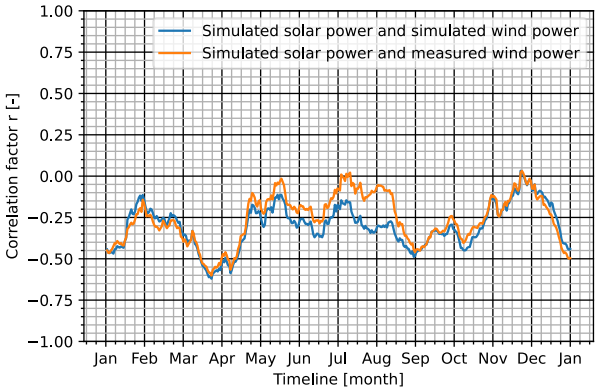

Figure 7.8: Correlation coefficient calculated at spans of 30 days for each day of the year using daily resolution.

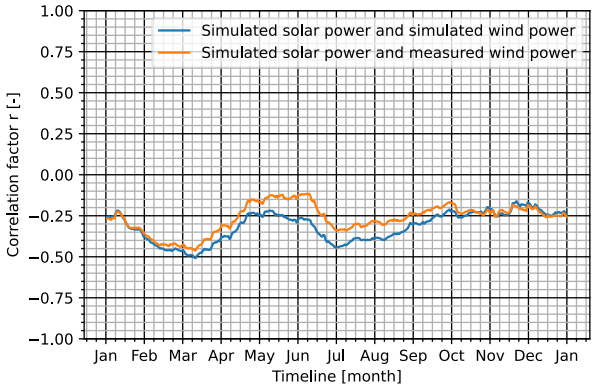

Figure 7.9: Correlation coefficient calculated at spans of 90 days for each day of the year using daily resolution.

8 Discussion

For the results in general, it is important to keep in mind that the period that has been considered is relatively short, being a period of four years from 2017 to 2020. This was done due to the period which measured wind power at Smøla is available. The following are some of the key results from the power production scenarios for the period 2017 to 2020, see Figure 5.1 for an overview with description of each scenario:

- Comparison scenario: The simulated wind power was 1633 GWh, while the measured wind power was 1357 GWh. The solar power produced for a 240 MWp solar farm was 725 GWh.
- Scenario 1: Gave a ratio of 67 % wind (150.4 MW) and 33 % solar (261 MWp) delivering 2174 GWh to Nordheim with curtailment at 114 GWh and an average transmission line usage of 43.0 %.
- Scenario 2: Gave a ratio of 74 % wind (170.2 MW) and 26 % solar (215 MWp) delivering 2250 GWh to Nordheim with curtailment at 118 GWh and an average transmission line usage of 44.6 %.
- Scenario 3: Only used wind power (172 MW) delivering 2824 GWh to Nordheim with curtailment at 140 GWh and an average transmission line usage of 56.0 %.
- Scenario 4: Gave a ratio of 85 % wind (160 MW) and 15 % solar (172 MWp) delivering 3105 GWh to Nordheim with curtailment at 163 GWh and an average transmission line usage of 61.5 %.
- Scenario 5: Gave a ratio of 85 % wind (272 MW) and 15 % solar (284 MWp) delivering 5345 GWh to Nordheim with curtailment at 281 GWh and an average transmission line usage of 62.0 %

The comparison scenario shows that the simulated wind power is overestimated by approximately 20 % and solar power produced at an installed capacity of 240 MWp seems comparable to the solar power produced in [4] given that a bifacial solar panel was used, which would produce slightly more power.

Scenario 1 presents the optimized installation of solar power for the current installation of wind turbines at Smøla given the constraints of 5 % curtailment and a 160 MVA transmission line capacity at 0.9 power factor. Scenario 3 and 4 presents the optimized scenarios for the larger capacity wind turbine without and with solar power given equal constraints as in Scenario 1. The results show that if Scenario1 is to be implemented in the near future with 261 MWp of solar capacity installed, then it may inhibit the potential wind power gained from a larger capacity wind turbine if curtailment is to be kept low or would need an expansion of the transmission line seeing as Scenario 4 resulted in 172 MWp of solar capacity installed. Going from Scenario 1 to Scenario 4 shows an increase in power delivered of 42.8 %, therefore a possible option to best utilize the wind power at Smøla for the future is to install solar capacity in the near future equivalent to the optimized scenario of installing a larger capacity wind turbine. Scenario 3 is also an option where only the larger wind turbines are installed which delivers 30 % more power than scenario 1 and delivers 10 % less power than scenario 4. Whether to install solar power or not from Scenario 3 to Scenario 4 is whether an additional 281 GWh power delivered with an increase in curtailment from 140 GWh to 163 GWh is worth it. This choice should also consider other topics such as economics or the need for a smoothing effect on power demand which has not been looked into in this report.

The ratio between wind and solar power in this report has varied between 67-85 % wind power with the remainder as solar power, which seems to coincide with the literature in Chapter 3 for Europe when balancing power is the focus with wind power having a larger share. However, for a future with only renewable energy sources the balance becomes more even with cited balance as 55-60 % wind power with the remainder as solar power, which includes energy storage solutions.

The reason for an increase in share of wind power compared to solar power when switching to a larger wind turbine can be attributed to the non-linear characteristics in power harvested from the following:

- Increasing the radius of the area swept by using larger rotor blades, increases the theoretical power that can be harvested as R^2, as given by equation (4.6).
- Increasing the height of the turbine can allow the turbine to capture wind with higher wind speeds and according to the theoretical power that can be harvested in equation (4.6) the wind speed W is given as W^3.

Another factor attributing significantly in this case is the increased performance given by the power curve of the SWT-4.0-130 wind turbine as shown in Figure 5.10 with lower wind speeds for cut-off wind speed W_c and rated wind speed W_r, while having equal furling wind speed W_f.

From viewing the study in [2] and [27], simply using the power curves to evaluate wind power production, which has been done in this report, may give very variable inaccuracies. The IEC-standard 61400-12-1 presents a recommended procedure for how manufacturers can produce power curves with corrections for turbulence intensity, wind shear, wind veer and so forth, which can then be used to assess power production. However, these power curves are often not freely available making comparisons difficult and the ones that exist are often without any reference to corrections represented in the power curve. [27] Therefore, many studies have focused on how to assess power curves, such as in in [2] and [27]. The methods presented in [2] uses a Gaussian filter that smooths out the power curve according to various parameters in order to emulate the effects of an actual wind farm, hence the model's name Virtual Wind Farm (VWF). The parametric model in [27] attempts to incorporate several environmental effects such as turbulence intensity into power curves, and the effects of turbulence intensity showcased in [27] shows a considerable smoothing of the power curve around the rated wind speed W_r. Therefore, when viewing the power curve of the SWT-4.0-130 in Figure 5.10, which has a relatively sharp power curve up to the rated wind speed W_r, it may be considered too ideal for a realistic situation leading to a possible further overestimation of wind power for Scenario 3 to 5.

Scenario 2 is simply an in between comparison to Scenario 4 showing the difference for the current installation of wind turbines if both installed capacities of solar and wind are considered variables. Scenario 5 shows the results by assuming that an equal amount of wind turbines currently at Smøla can be installed for the larger capacity wind turbine in the same area by increasing the transmission line limit to 245 MW in order to keep the curtailed power below 5 %. The result in Scenario 5 is particularly susceptible to interference between wind turbines, also known as wake effects, which has not been considered in this report and as mentioned in [27] may cause losses of 11-13 % within 7-9 rotor diameters of the turbine. A spacing of 7-9 rotor diameters for the larger capacity wind turbine (130 m) results in a spacing of 910-1170 meters, and considering the current row spacing of 700-1000 meter and spacing in the rows of 240-350 meters [14] can contribute to considerable losses, which are highly variable depending on wind direction. Scenario 5 also shows that increasing the transmission line limit does not significantly affect the balance between wind and solar power, nor the average transmission line usage.

The results from the correlation analysis in Table 7.4 shows that the correlation factor for hourly, daily and monthly resolution is generally more positive for simulated solar power with measured wind power than with simulated wind power. The effect of this difference can be seen from the results in Table 7.1, where even though more power was produced for simulated solar and wind power as compared with measured wind power, less power was curtailed as a result. This result could also present errors in the balance between solar and wind power for the optimized scenarios. In the figures from Figure 7.6 to Figure 7.9 the correlation factor has been calculated at every day of the year at hourly and daily resolution with spans of 30 and 90 days. These figures shows that it is approximately during the months of May to August where the correlation factor between simulated solar power, with either simulated or measured wind power deviates the most.

As for the correlation values themselves, at hourly resolution they vary between -0.01 to -0.22, with the correlation across the year being on average -0.15, indicating very low negative correlation on average to no correlation at times. At daily resolution the correlation factor varies between -0.08 to -0.53, with correlation across the year being on average -0.34. The correlation across the year indicates still a somewhat low negative correlation, which is very much affected by the months of November and December for both cases, and for simulated solar and measured wind power the months of July and August are also quite low. At monthly resolution the correlation factors are only calculated across the year once and resulted in an average of -0.58, which can be considered a moderate negative correlation. Overall, the results show that the complementary characteristics of co-locating solar and wind is strongest when considering a monthly timeline and gets weaker as the resolution increases to daily and weaker again for hourly resolution. For the hourly and the daily resolution the figures in Figure 7.6 to Figure 7.9 show that the negative correlation is generally stronger during the periods January-April and August-October, which could be relevant depending on which time of the year a smoothing effect between solar and wind is desired.

When compared to correlation analysis between solar and wind from literature presented in Chapter 3, the same pattern is observed for an increasing negative correlation when going from hourly to daily and daily to monthly resolution. The strength of the negative correlation is comparable to the Pearson's r correlation coefficients found for Tromsø in [24] and is noticeably weaker than the correlation values found for Sweden on a national scale in [15].

9 Conclusion

This report has looked into the complementary characteristics of co-locating solar and wind power at Smøla, Norway. This has been done by evaluating power production scenarios by choosing a larger capacity wind turbine and finding the optimal mix of solar and wind power that maximizes the usage of the transmission line capacity. It has also been evaluated based on a correlation analysis using the Pearson's r correlation factor. Both the power production scenarios and the correlation analysis has been performed for the time period 2017-2020.

The power production scenarios found that:

- Only installing the larger capacity wind turbine resulted in a power delivered to Nordheim of 2824 GWh and an average transmission line capacity usage of 56.0 %, with 140 GWh of power being curtailed.
- Co-locating solar and wind power resulted 3105 GWh of power being delivered to Nordheim, where the power produced constituted of 85 % wind power and 15 % solar power. The average transmission line capacity usage was 61.5 % and 163 GWh of power was curtailed.

The produced wind power is estimated to have a 20 % overestimation due to the difference between simulated and measured wind power, with a possible further overestimation for the larger capacity wind turbine due to the possibility of its power curve being too ideal for environmental effects in a realistic situation.

The correlation analysis shows that the strength of the negative correlation factors increases when resolution of the data is changed from hourly to daily and from daily to monthly. The correlation factor calculated across the entire year was -0.15 at hourly, -0.34 for daily and -0.58 for monthly resolution. Suggesting that co-locating solar and wind power sees the biggest benefit at monthly timelines in terms of complementing each other, so that when either of them decreases the other tends to increase. A difference in correlation strength is also observed for simulated solar power with either simulated or measured wind power, which can also contribute to error in the optimal mixing of solar and wind power in the power production scenarios.

Future Work

Produced more accurate results for assessing power production at Smøla from solar and wind power by using on-site measurements of irradiance and wind speeds, and by assessing corrections for power curves of wind turbines due to external/environmental factors.

References

[1] S. Pfenninger and I. Staffell, “Long-term patterns of European PV output using 30 years of validated hourly reanalysis and satelitte data,” Energy, Volume 114, pp 1251-1265, Elsevier, Amsterdam, Netherlands, 2016, doi.org/10.1016/j.energy.2016.08.060.

[2] I. Staffell and S. Pfenninger, “Using bias-corrected reanalysis to simulate current and future wind power output,” Energy, Volume 114, pp. 1224-1239, Elsevier, Amsterdam, Netherlands, 2016, doi.org/10.1016/j.energy.2016.08.068.

[3] Reneawbles.ninja, [Online]. Available: www.renewables.ninja/. [Accessed 13 03 2023].

[4] COWI and IFE, “Utredning solenergi Smøla (Study of solar energy at Smøla),” COWI, Oslo, Norway, https://mrfylke.no/content/download/27693/279314, 2023.

[5] Photovoltaic Geographical Information System - PVGIS, [Online]. Available: https://re.jrc.ec.europa.eu/pvg_tools/en/. [Accessed 13 03 2023].

[6] Photovoltaic Geographical Information System - PVGIS, [Online]. Available: https://joint-research-centre.ec.europa.eu/pvgis-online-tool/getting-started-pvgis/pvgis-data-sources-calculation-methods_en. [Accessed 26 03 2023].

[7] T. Huld, G. Friesen, A. Skoczek, R. P. Kenny, T. Sample, M. Field and E. D. Dunlop, “A power-rating model for crystalline silicon PV modules,” Elsevier B. V., Amsterdam, Netherlands, 2011, doi.org/10.1016/j.solmat.2011.07.026.

[8] G. Thorsnæs, “Store Norske Leksikon,” 27 01 2023. [Online]. Available: snl.no/Smøla. [Accessed 13 03 2023].

[9] StevenJothen, “Wikipedia Commons,” 23 04 2009. [Online]. Available: https://commons.wikimedia.org/wiki/File:Norway_Counties_Møre_og_Romsdal_Position.svg. [Accessed 13 03 2023].

[10] Statens Vegvesen, “Statens Vegvesen - Vegkart,” 03 03 2023. [Online]. Available: https://vegkart.atlas.vegvesen.no. [Accessed 13 03 2023].

[11] OpenStreetMap, [Online]. Available: openstreetmap.org. [Accessed 13 03 2023].

[12] Statkraft, 09 2011. [Online]. Available: https://www.statkraft.com/globalassets/old-contains-the-old-folder-structure/documents/faktaark-smola-wind-farm-eng-sept-2011_tcm9-17664.pdf. [Accessed 13 03 2023].

[13] TheWindPower, [Online]. Available: https://www.thewindpower.net/windfarm_en_746_smola.php. [Accessed 13 03 2023].

[14] Nexans, “nexans.no,” [Online]. Available: https://www.nexans.no/no/segments/infrastructure-land/Wind-onshore/Smola-Wind-farm.html. [Accessed 14 05 2023].

[15] J. Widén, “Correlations Between Large-Scale Solar and Wind Power in a Future Scenario for Sweden,” IEEE Transactions on Sustainable Energy, vol. 2, no. 2, pp. 177-184, IEEE, New York City, U.S., 2011, doi: 10.1109/TSTE.2010.2101620.

[16] J. Widén, N. Carpman, V. Castellucci, D. Lingfors, J. Olauson, F. Remouit, M. Bergkvist, M. Grabbe and R. Waters, “Variability assesment and forecasting of renewables: A review for solar, wind, wave and tidal resources,” Renewable and Sustainable Energy Reviews, Volume 44, pp. 356-375, Elsevier , Amsterdam, Netherlands, 2015, doi.org/10.1016/j.rser.2014.12.019.

[17] O. Lindberg, D. Lingfors, J. Arnqvist, D. v. d. Meer and J. Munkhammar, “Day-ahead probabilistic forecasting at a co-located wind and solar power park in Sweden: Trading and forecast verification,” Advances in Applied Energy, Volume 9, Elsevier, Amsterdam, Netherlands, 2023, doi.org/10.1016/j.adapen.2022.100120.

[18] C. Bozonnat and C. A. Schlosser, “Characterization of the Solar Power Resource in Europe and Assesing Benefits of Co-location with Wind Power Installations,” Massachusetts Institute of Technology - MIT, Cambridge, Massachusetts, 2014.

[19] G. G. Dranka, P. Ferrerira and A. I. F. Vaz, “A review of co-optimization approaches for operational and planning problems in the energy sector,” Applied Energy, Volume 304, Elsevier, Amsterdam, Netherlands, 2021, doi.org/10.1016/j.apenergy.2021.117703.

[20] P. E. Bett and H. E. Thornton, “The climatological relationships between wind and solar energy supply in Britain,” Renewable Energy, Volume 87, Part 1, pages 96-110, Elsevier , Amsterdam, Netherlands, 2016, doi.org/10.1016/j.renene.2015.10.006.

[21] W. Zappa and M. v. d. Broek, “Analysing the potential of integrating wind and solar power in Europe using spatial optimization under various scenarios,” Renewable and Sustainable Energy Reviews, Volume 94, pp 1192-1216, Elsevier, Amsterdam, Netherlands, 2018, doi.org/10.1016/j.rser.2018.05.071.

[22] D. Heide, M. Greiner, L. v. Bremen and C. Hoffman, “Reduced storage and balancing needs in a fully renewable European power system with excess wind and solar power generation,” Renewable Energy, Volume 36, Issue 9, pp 2515-2523, Elsevier, Amsterdam, Netherlands, 2011, doi.org/10.1016/j.renene.2011.02.009.

[23] D. Heide, L. v. Bremen, M. Greiner, C. Hoffman, M. Speckmann and S. Bofinger, “Seasonal optimal mix of wind and solar power in a future, highly renewable Europe,” Renewable Energy Volume 33, Issue 11, pp 2483-2489, Elsevier, Amsterdam, Netherlands, 2010, doi.org/10.1016/j.renene.2010.03.012.

[24] K. Solbakken, B. Babar and T. Bostrôm, “Correlation of wind and solar power in high-latitude artic areas in Northern Norway and Svalbard,” Renwe. Energy Enviro. Sustain, Volume 1, Issue 42, EDP sciences, Les Ulis, France, 2016, doi.org/10.1051/rees/2016027.

[25] “Assessing complementarity of wind and solar resources for energy production in Italy. A Monte Carlo approach,” Renewable Energy Volume 63, pp 576-586, Elsevier,

Amsterdam, Netherlands, 2014, doi-org.ezproxy2.usn.no/10.1016/j.renene.2013.10.028.

[26] MathWorks, “se.mathworks.com,” [Online]. Available: https://se.mathworks.com/products/demos/symbolictlbx/wind-turbine-power.html. [Accessed 12 03 2023].

[27] R. B. Yves-Marie Saint-Drenan, M. Jansen, I. Staffell, A. Troccoli, L. Dubus, J. Schimdt, K. Gruber, S. G. Simöes and S. Heier, “A parametric model for wind turbine power curves incorporating enviromental conditions,” Renewable Energy, Volume 157, pp. 754-768, Elsevier, Netherlands, Amsterdam, 2020, doi.org/10.1016/j.renene.2020.04.123.

[28] M. Stojiljkovi, “realpython.com,” [Online]. Available: https://realpython.com/numpy-scipy-pandas-correlation-python/. [Accessed 11 03 2023].

[29] TheWindPower, [Online]. Available: https://www.thewindpower.net/index.php. [Accessed 23 02 2023].

[30] Siemens AG, 2015. [Online]. Available: https://pdf.directindustry.com/pdf/siemens-gamesa/siemens-g4-platform/102147-425695-_2.html. [Accessed 24 04 2023].

[31] Siemens AG, 2015. [Online]. Available: https://pdf.directindustry.com/pdf/siemens-gamesa/introducing-swt-23-120/102147-642452-_2.html. [Accessed 24 04 2023].

[32] Siemens Gamesa, “siemensgamesa.com,” 02 2023. [Online]. Available: https://www.siemensgamesa.com/en-int/-/media/siemensgamesa/downloads/en/products-and-services/onshore/brochures/siemens-gamesa-wind-turbine-4-x-platform-brochure-en.pdf. [Accessed 24 04 2023].

Appendices

Appendix A – Project description:

University of South-Eastern Norway

Faculty of Technology, Natural Sciences and Maritime Sciences, Campus Porsgrunn

FMH606 Master's Thesis

Title: Solar Power in Wind Power Park - Evaluating flexible power generation based on real and simulated data from Statkraft Smøla Wind Park.

USN supervisor: Nils Jakob Johannesen, Ass. Prof. USN

Exterior partner: Bjarne Tufte, Section Head, COWI

Task background:
The Smøla wind park has a total of 68 turbines and 150 MW installed power that produce an annual output of 356 GWh, enough to supply 17,800 Norwegian households with electricity. The wind farm is in flat and open terrain 10-40 meters above sea level. Statkraft is planning to option for flexible operation by installing an additional 150 MW solar power. To evaluate the flexible operation a digital twin is produced. The digital twin, which will be a virtual copy of a solar farm located inside the wind farm on Smøla, will simulate the potential for electricity production in an energy park that combines wind and solar energy.

Task description:
Analyse how the network capacity in the area affects the development of solar power in interaction with wind power and evaluate net-scenarios based on correlation analysis.

Progress:

- Literature Survey
- Modeling and Simulation of Wind Solar Hybrid System using Python or Matlab/Simulink
- Theoretisize the digital twin.
  Analytical:
- Analyse different alternatives based on the the simulated model
- Compare these findings with the findings in the Digital twin

Student category: EPE

Is the task suitable for online students (not present at the campus)? Yes
Supervision:
As a general rule, the student is entitled to 15-20 hours of supervision. This includes necessary time for the supervisor to prepare for supervision meetings (reading material to be discussed, etc).

Signatures:
1.2.23
Supervisor (date and signature):

Student (write clearly in all capitalized letters):
ANDREAS DOLVEN JACOBSEN
Student (date and signature):
01.02.2023 Andreas D. Jacobsen